Journal of Sound and Vibration (2002) **257**(2), 207–246
doi:10.1006/jsvi.5055, available online at http://www.idealibrary.com on IDEAL®

A NOVEL APPROACH FOR THE ANALYSIS OF HIGH-FREQUENCY VIBRATIONS

G. W. Wei

Department of Mathematics, Michigan State University, East Lansing, MI 48824-1027, *U.S.A.*
Department of Computational Science, National University of Singapore, Singapore 117543, *Singapore.*
E-mail: cscweigw@nus.edu.sg

Y. B. Zhao

Department of Computational Science, National University of Singapore, Level 7, *Block S*17 3 *Science Drive, Singapore* 117543, *Singapore*

AND

Y. Xiang

School of Engineering and Industrial Design, University of Western Sydney, Penrith South DC, NSW 1797, *Australia*

(*Received* 25 *May* 2001, *and in final form* 28 *November* 2001)

Despite much effort in the past few decades, the numerical prediction of high-frequency vibrations remains a challenging task to the engineering and scientific communities due to the numerical instability of existing computational methods. However, such prediction is of crucial importance to certain problems of pressing practical concern, as pointed out by Langley and Bardell (1998 *The Aeronautical Journal* **102**, 287–297). This paper introduces the discrete singular convolution (DSC) algorithm for the prediction and analysis of high-frequency vibration of structures. Both a beam and two-span plates are employed as test examples to demonstrate the capability of the DSC algorithm for high-frequency vibration analysis. A completely independent approach, the Levy method, is employed to provide exact solutions for a cross validation of the proposed method. The reliability of the DSC results is also validated by convergence studies. Remarkably, extremely accurate and stable results are obtained in this work, e.g., the relative DSC errors for the first 7100 modes of the beam and the first 4500 modes of the two-span plates are all $<1\%$. No numerical instability is encountered in the present study.

1. INTRODUCTION

The prediction and control of high-frequency vibrations is of crucial importance to aerospace structures such as aircraft, rotocraft, satellite and space shutter, and many defence equipments such as jet fighter, rocket, missile, etc. Typically, these man-made structures are constantly subjected to various forms of high-frequency excitation which may arise from either mechanical or acoustical sources such as jet noise, propeller noise, rotor noise, and combustion turbulence from an engine. Structural response to external excitation can lead to either on-resonance (i.e., forced vibration) or fast energy dissipation (i.e., heat production). Sometimes, undesired self-excited vibration occurs under a sustainable mechanical load or stress. Excessive vibration and unacceptable noise create great fluctuation of mechanical loads and stress, and lead to fatigue failure of structural

0022-460X/02/$35.00

components, loosening of threaded connection, friction and wear, and damage of electronic and other delicate components. Therefore, there is clearly a need for the prediction and control of the high-frequency vibration and noise levels at the structural design stage and this in turn requires the availability of analysis methods which are able to predict the structural dynamic response. However, developing accurate and numerically stable methods for the analysis of high-frequency vibration is an extremely challenging task owing to the numerical instability in existing methods [1].

The most popular method used in structural analysis is the conventional finite element method (FEM), or the *h*-version FEM, which is commercially available for structural design. Usually, basis function of low order approximations is used in *h*-version FEM and the convergence is sought by successive refinement of the mesh. Unfortunately, such a refinement is computationally too expensive for capturing high-frequency vibrations. Although the *h*-version FEM is adequate for low-frequency vibration analysis, it is not well-suited to the vibration analysis of medium- or high-frequency regimes [1].

The *p*-version of the FEM is later developed in which the convergence is sought by increasing the degree of polynomials with a fixed mesh. This method permits modal refinement without having to remesh the computational domain and generally offers superior performance in the *h*-version FEM for the vibration analysis of higher frequencies. Due to the additional requirement of boundary conditions in the analysis, it is more efficient to construct the so-called hierarchical polynomial basis which has the property that the set of basis functions corresponding to a polynomial approximation of order p constitutes a subset of the set of basis functions corresponding to a polynomial approximation of order $p+1$ [2, 3]. For example, Zhu [2] proposed the following modified Legendre polynomial:

$$Z_m^s(x) = \sum_{n=0}^{m/2} \frac{(-1)^n (2m-2n-2s-1)!!}{2^n n!} \frac{}{(m-2n)!} x^{m-2n}, \tag{1}$$

which is a hierarchical shape function of C^{s-1} continuity. Bardell [3] built a hierarchical shape function by considering $s=2$. His first four terms are given by

$$B_1(x) = \tfrac{1}{2} - \tfrac{3}{4}x + \tfrac{1}{4}x^3, \qquad B_2(x) = \tfrac{1}{8} - \tfrac{1}{8}x - \tfrac{1}{8}x^2 + \tfrac{1}{8}x^3,$$

$$B_3(x) = \tfrac{1}{2} - \tfrac{3}{4}x + \tfrac{1}{4}x^3, \qquad B_4(x) = -\tfrac{1}{8} - \tfrac{1}{8}x + \tfrac{1}{8}x^2 + \tfrac{1}{8}x^3. \tag{2}$$

Higher order polynomials are constructed from Zhu's expression (1)

$$B_r(x) = Z_{m=r-1}^{s=2}(x), \quad r > 4. \tag{3}$$

Bardell has demonstrated the success of this shape function for structural analysis. However, as analyzed in details by Beslin and Nicolas [4], for high-frequency vibrations, Bardell's polynomials are easily subject to numerical instability, caused by the computer round-off error in handling high-degree polynomials.

Rayleigh–Ritz and Ritz methods are akin to the *p*-version FEM in the selection of basis functions. This type of methods utilize the Ritz variational principle to formulate a solution to the problem of structural analysis. They have been extensively studied recently and have a proven success for a variety of tasks in the analysis of solid mechanics problems [5, 6]. However, like the *p*-version FEM, the Ritz type of methods suffer from numerical instability in the prediction of high-frequency vibrations.

The Levy method is an interesting approach for vibration analysis. It takes an analytical solution form, i.e., trigonometric sine functions, for a rectangular plate along simply

supported two parallel edges and allows an arbitrary combination of edge conditions in the two remaining edges. In principle, the Levy method is capable of providing exact solutions for the prediction of very high-frequency vibration of rectangular plates. However, its practical use is hindered by the geometric requirement.

Due to the difficulty encountered by conventional numerical methods for high-frequency analysis, a few alternative approaches have been proposed, including dynamic stiffness (continuous element) method [7, 8], periodic structure approximation [9, 10], statistical energy analysis [11, 12] and wave intensity analysis [13]. The dynamical stiffness method has been successfully used for the analysis of one-dimensional structures. But the method essentially treats an idealized structure when applied to a complex two-dimensional structure. Idealized periodicity is assumed in the periodic structure theory, and such periodicity might never exactly occur in real-world structures. Statistical energy analysis does not predict detailed high-frequency modes. Instead, it attempts to provide the spatial frequency distribution of a structure. Such information is valuable for estimating the frequency response of a structure under external noise. As a generalization of the statistical energy analysis, wave intensity analysis does not assume a diffusive vibration wave field. In fact, the last three approaches treat the original physical system in a manner which might differ from the actual mechanical model.

The most promising approach of high-frequency vibration analysis was recently proposed by Beslin and Nicolas [4]. Their method utilizes Fourier type trigonometric function set $\{\phi(x)\}$ of the form

$$\phi_r(x) = \sin(a_r x + b_r)\sin(c_r x + d_r), \quad r = 1, 2, \ldots \tag{4}$$

as basis functions to achieve element p enrichment. Here, the coefficients a_r, b_r, c_r and d_r are chosen appropriately [4] to satisfy the boundary conditions of a plate. A variety of results were presented to demonstrate the numerical capability of the method in predicting the flexural natural frequencies. They found that this method gave good convergence at medium-frequency range but poor convergence at low frequencies. Remarkably, such a hierarchical FEM works much better than the hierarchical FEM of Bardell [3] for high-frequency analysis and was devised to predict the 850th mode for an all-edge simply supported rectangular plate and the 820th mode for an all-edge free plate with errors being $<2\%$. These, in fact, are the best available result in the literature and give a clear indication of the potential of their method to penetrate the medium-frequency regime. However, as illustrated by Beslin and Nicolas [4], a significant numerical error occurs on sets beyond the 850th mode in a 1024 basis function simulation due to numerical instability.

In summary, despite much effort in the past few decades, the numerical prediction of high-frequency vibrations remains a challenging task to the engineering and scientific communities. It is pertinent to quote Professors Langley and Bardell [1] from their recent review paper: "... the prediction of medium to high frequency vibration levels is a particularly difficult task. ... there is no single technique which can be applied with confidence to all types of aerospace structures. Furthermore, there are certain problems of pressing practical concern for which it is not possible at present to make a reliable design prediction of high frequency vibration levels—the prediction of on-orbit micro-vibration levels in satellite structures is arguably a problem of this type."

The purpose of this paper is to introduce a novel computational method, the discrete singular convolution (DSC) [14–16], for the prediction and control of high-frequency vibrations of beams and two-span plates. Singular integrations often occur in science and engineering and their most common forms include singular kernels of Hilbert, Abel and delta types. The DSC is a new, successful approach for numerical implementation of

singular integrations. The mathematical foundation of the DSC algorithm is the theory of distributions [17] and the theory of wavelets. In the DSC algorithm, numerical solutions of differential equations are formulated via the singular kernels of delta type. Specifically, both *bandlimited reproducing kernels* and *approximate reproducing kernels* are constructed as the sequences of approximations to the *universal reproducing kernel*, the delta distribution. By appropriately selecting parameters in a DSC kernel, the DSC approach exhibits controllable accuracy for integration and shows excellent flexibility in handling complex geometries and boundary conditions. It was demonstrated [15] that different implementations of the DSC algorithm, such as global, local, Galerkin, collocation, and finite difference, can be deduced from a single starting point. Thus, the DSC algorithm provides a unified representation to these numerical methods. The DSC has been successfully applied to the numerical solution of the Fokker–Planck [14, 15] and the Schrödinger equations [18]. It achieves machine precision in solving the Taylor problem, the Navier–Stokes equation [19] with incompressible constraint and periodic boundary conditions. It is also used to facilitate a novel synchronization scheme for shock capturing [20]. Recently, the DSC algorithm was used to integrate the Cahn–Hilliard equation in a circular domain [21] and the sine-Gordon equation with the initial values close to a homoclinic manifold singularity [22], for which conventional local methods encounter great difficulties and result in numerically induced chaos [23]. The work that is most relevant to the present study is the use of DSC for plate [24, 25] and beam [26] analyses. The DSC algorithm was utilized to estimate the first 100 modes of a simply supported square plate with at least 11 significant figures [24, 25]. Most recently, we illustrated that the DSC provides excellent results of plates with mixed boundary condition [27] and internal supports [28]. A preliminary investigation indicates that the DSC algorithm works very well for the high-frequency analysis of plates with simply supported and clamped edges [29]. In this paper, we demonstrate that the DSC algorithm is capable of giving extremely accurate prediction of thousands of vibration modes for both beam and two-span plates without encountering any difficulty of numerical instability. Plates with internal support is used as an example to illustrate DSC ability for vibration control. A completely independent approach, the Levy method, is employed for a cross validation of the DSC results.

The organization of the paper is as follows. Theory and algorithm for beam and plate analyses are given in section 2. For the sake of integrity, we briefly review the computational philosophy of the DSC algorithm and the Levy approach. The prediction of high-frequency vibrations of beam and plates is presented in section 3. The ability of vibration control is exemplified by plates with internal line supports. The validity and accuracy of the DSC method for higher frequency vibration analysis are verified by convergence studies, error analyses and by comparison with the Levy solutions. Case studies are performed on various combinations of different boundary and internal support conditions. Extensive frequency parameters are tabulated for two-span plates of six distinct edge support conditions obtained as a combination of simply supported and clamped edges. A conclusion is given in section 4.

2. THEORY AND ALGORITHM

The problem of beam and plate vibrations is described below. For integrity and convenience, both the DSC and Levy methods are briefly reviewed in this section. However, the reader is referred to the original work for more detailed information [5, 14–16]. The analytical model for a simply supported beam, the DSC algorithm and the Levy method for plate analysis are presented in this section.

2.1. VIBRATION OF BEAM AND PLATE

2.1.1. *The beam problem*

The natural vibration of a beam of uniform flexural rigidity, subjected to either tensile or compressive axial forces whose magnitude is below the value of the so-called Euler elastic buckling critic, can be formulated as an eigenvalue problem [30]

$$\frac{\mathrm{d}^4 B(x)}{\mathrm{d}x^4} + \frac{S}{EI}\frac{\mathrm{d}^2 B(x)}{\mathrm{d}x^2} = k^2 \frac{mA}{EI} B(x), \quad x \in [0, a], \tag{5}$$

with simply supported boundary condition

$$B(0) = \frac{\mathrm{d}^2 B(0)}{\mathrm{d}x^2} = 0, \qquad B(a) = \frac{\mathrm{d}^2 B(a)}{\mathrm{d}x^2} = 0, \tag{6}$$

where a is the length of the beam, a positive S represents the magnitude of a compressive force and a negative S represents the magnitude of a tensile force, m and A are the mass density of the material and the cross-sectional area of the beam respectively. This problem is also analytically soluble and its exact solutions have the form

$$B_n(x) = b_n \sin\left(\frac{n\pi x}{a}\right), \quad n = 1, 2, \ldots, \tag{7}$$

where b_n is an arbitrary constant and $B_n(x)$ satisfies all of the boundary conditions in equation (6). A set of eigenvalues are given by

$$k_n^2 \frac{mA}{EI} = \left(\frac{n\pi}{a}\right)^4 - \frac{S}{EI}\left(\frac{n\pi}{a}\right)^2. \tag{8}$$

To ensure the statement of an eigenvalue problem, the compressive force is required to be bounded from above. For free vibration problem ($S = 0$), the above formulation still stands.

2.1.2 *The plate problem*

Although we limit our attention to the vibration of rectangular (classic) Kirchhoff plates with simply supported and clamped edges, the method can be used for many other applications in solid mechanics. Let us consider a rectangular plate of length a, width b, thickness h, mass density ρ, modulus of elasticity E, and the Poisson ratio v. The origin of the Cartesian co-ordinates (x, y) is set at the lower left corner of the plate. The governing differential equation for the plate is given by [31]

$$\frac{\partial^4 w}{\partial x^4} + 2\frac{\partial^4 w}{\partial x^2 \partial y^2} + \frac{\partial^4 w}{\partial y^4} = \frac{\rho h \omega^2}{D} w, \tag{9}$$

where $w(x, y)$ is the transverse displacement of the midsurface of the plate, $D = Eh^3/[12(1 - v^2)]$ the flexural rigidity, and ω the circular frequency. We consider one of the following two types of support conditions for each plate edge:

For simply supported edge (*S*):

$$w = 0, \quad -D\left(\frac{\partial^2 w}{\partial n^2} + v\frac{\partial^2 w}{\partial s^2}\right) = 0. \tag{10}$$

For clamped edge (*C*):

$$w = 0, \qquad \frac{\partial w}{\partial n} = 0, \tag{11}$$

where n and s denote the normal and tangential co-ordinates with respect to the rectangular plate edge respectively.

It is noted that the objective of this paper is to explore the utility of the DSC algorithm in dealing with high-frequency vibrations. To this end, two simple physical models, i.e., beams and thin plates, are chosen so that additional complexity from more complicated models is avoided. Nevertheless, from the physical point of view, the plate and beam theories used in this study may not be strictly valid in predicting the very high-frequency vibration of real plates and beams. For example, if a plate vibrates in very high-frequency, the wavelength of a vibration mode may be comparable or even smaller than the thickness dimension of the plate. In such a case, rotary inertia and shear deformation may have significant influence on the vibration behavior of the plate. Either the first order plate theory (the Mindlin plate theory [32]), the higher order plate theory (the Reddy plate theory [33]) or the three-dimensional (3-D) theory for solid structures can be employed for achieving a better approximation. It is definite that the DSC algorithm introduced in the present work can be easily adopted for solving the problem of high-frequency analysis in association with other structural theories.[†]

2.2. DISCRETE SINGULAR CONVOLUTION

Singular convolutions (SC) are a special class of mathematical transformations, which appear in many science and engineering problems, such as Hilbert, Abel and Radon transforms. It is most convenient to discuss the singular convolution in the context of the theory of distributions. The latter has a significant impact in mathematical analysis. Not only it provides a rigorous justification for a number of informal manipulations in physical and engineering sciences, but also it opens a new area of mathematics, which in turn gives impetus to many other mathematical disciplines such as operator calculus, differential equations, functional analysis, harmonic analysis, and transformation theory. In fact, the theory of wavelets and frames, a new mathematical branch developed in recent years, can also find its root in the theory of distributions.

Let T be a distribution and $\eta(t)$ be an element of the space of test functions. A singular convolution is defined as

$$F(t) = (T * \eta)\,(t) \;= \int_{-\infty}^{\infty} T(t-x)\,\eta(x)\,\mathrm{d}x. \tag{12}$$

Here, $T(t-x)$ is a singular kernel. Depending on the form of the kernel T, the singular convolution is the central issue for a wide range of science and engineering problems. For example, the singular kernels of Hilbert type have a general form of

$$T(x) = \frac{1}{x^n} \quad (n = 1, 2, \ldots). \tag{13}$$

[†] For example, the present method gives absolute errors of 10^{-8} or less for all the first 100 modes of a simply supported Mindlin plate by using 31^2 grid points.

Here, kernel $T(x) = 1/x$ commonly occurs in electrodynamics, theory of linear response, signal processing, theory of analytic functions, and the Hilbert transform. When $n = 2$, $T(x) = 1/x^2$ is the kernel used in tomography. Another interesting example is the singular kernels of the Abel type

$$T(x) = \frac{1}{x^\beta} \quad (0 < \beta < 1). \tag{14}$$

These kernels can be recognized as the special cases of the singular integral equations of the Volterra type of the first kind. The singular kernels of Abel type have applications in the area of holography and interferometry with phase objects (of practical importance in aerodynamics, heat and mass transfer, and plasma diagnostics). They are intimately connected with the Radon transform, for example, in determining the refractive index from the knowledge of a holographic interferogram. The other important example is the singular kernels of delta type

$$T(x) = \delta^{(n)}(x) \quad (n = 0, 1, 2, \dots). \tag{15}$$

Here, kernel $T(x) = \delta(x)$ is of particular importance for the interpolation of surfaces and curves (including atomic, molecular and biological potential energy surfaces, engineering surfaces and a variety of image-processing and pattern-recognition problems involving low-pass filters). Higher order kernels, $T(x) = \delta^{(n)}(x)$, $(n = 1, 2, \dots)$ are essential for numerically solving partial differential equations and for image processing, noise estimation, etc. However, since these kernels are singular, they cannot be directly digitized in computers. Hence, the singular convolution, equation (12), is of little numerical merit. To avoid the difficulty of using singular expressions directly in computer, we construct sequences of approximations $\{T_\alpha\}$ to the distribution T

$$\lim_{\alpha \to \alpha_0} T_\alpha(x) \to T(x), \tag{16}$$

where α_0 is a generalized limit. Obviously, in the case of $T(x) = \delta(x)$, each element in the sequence, $T_\alpha(x)$, is a delta sequence kernel. Note that one retains the delta distribution at the limit of a delta sequence kernel. Computationally, the Fourier transform of the delta distribution is unity. Hence, it is a *universal reproducing kernel* for numerical computations and an *all-pass filter* for image and signal processing. Therefore, the delta distribution can be used as a starting point for the construction of either band-limited reproducing kernels or approximate reproducing kernels. However, exact reproducing kernels have bad localization in the time (spatial) domain, whereas approximate reproducing kernels can be localized in both time and frequency representations. Furthermore, with a sufficiently smooth approximation, it is useful to consider a *discrete singular convolution* (DSC)

$$F_\alpha(t) = \sum_k T_\alpha(t - x_k)\, f(x_k), \tag{17}$$

where $F_\alpha(t)$ is an approximation to $F(t)$ and $\{x_k\}$ is an appropriate set of discrete points on which the DSC, equation (17), is well defined. Note that, the original test function $\eta(x)$ has been replaced by $f(x)$. The mathematical property or requirement of $f(x)$ is determined by the approximate kernel T_α. In general, the convolution is required being Lebesgue integrable.

The delta distribution or the so-called Dirac delta function (δ) is a generalized function which is integrable inside a particular interval but in itself need not have a value. It is given as a continuous linear functional on the space of test functions, $\mathscr{D}(-\infty, \infty)$,

$$\langle \delta, \phi \rangle = \delta(\phi) = \int_{-\infty}^{\infty} \delta\phi = \phi(0). \tag{18}$$

A delta sequence kernel, $\{\delta_\alpha(x)\}$, is a sequence of kernel functions on $(-\infty, \infty)$ which is integrable over every compact domain and their inner product with every test function ϕ converges to the delta distribution

$$\lim_{\alpha \to \alpha_0} \int_{-\infty}^{\infty} \delta_\alpha \phi = \langle \delta, \phi \rangle, \tag{19}$$

where the (real or complex) parameter α approaches α_0, which can either be ∞ or a limit value, depending on the situation (such a convention for α_0 is used throughout this paper). If α_0 represents a limit value, the corresponding delta sequence kernel is a fundamental family. Depending on the explicit form of δ_α, the condition on ϕ can be relaxed. For example, if δ_α is given as

$$\delta_\alpha(x) = \begin{cases} \alpha & \text{for } 0 < x < 1/\alpha,\ \alpha = 1, 2, \ldots, \\ 0 & \text{otherwise,} \end{cases} \tag{20}$$

then equation (19) makes sense for every ϕ in $C(-\infty, \infty)$.

There are many delta sequence kernels arising in the theory of partial differential equations (PDE), Fourier transforms and signal analysis, with completely different mathematical properties. The delta sequence kernels of the Dirichlet type have very distinct mathematical properties and have been used in the present work. Let $\{\delta_\alpha\}$ be a sequence of functions on $(-\infty, \infty)$ which are integrable over every bounded interval. We call $\{\delta_\alpha\}$ a delta sequence kernel of Dirichlet type if

1. $\int_{-a}^{a} \delta_\alpha \to 1$ as $\alpha \to \alpha_0$ for some finite constant a.
2. For every constant $\gamma > 0$; $(\int_{-\infty}^{-\gamma} + \int_{\gamma}^{\infty})\, \delta_\alpha \to 0$ as $\alpha \to \alpha_0$.
3. There are positive constants C_1 and C_2 such that

$$|\delta_\alpha(x)| \leqslant \frac{C_1}{|x|} + C_2$$

for all x and α.

Shannon's delta sequence kernel (or Dirichlet's continuous delta sequence kernel) is one of the most important examples of the delta sequence kernel of Dirichlet type and is given by the following (inverse) Fourier transform of the characteristic function, $\chi_{[-\alpha/2\pi, \alpha/2\pi]}$,

$$\begin{aligned} \delta_\alpha(x) &= \int_{-\infty}^{\infty} \chi_{[-\alpha/2\pi, \alpha/2\pi]}\, \mathrm{e}^{-\mathrm{i}2\pi\xi x}\, \mathrm{d}\xi \\ &= \frac{\sin(\alpha x)}{\pi x}. \end{aligned} \tag{21}$$

Alternatively, Shannon's delta sequence kernel can be given as an integration

$$\delta_\alpha(x) = \frac{1}{\pi}\int_0^\alpha \cos(xy)\,\mathrm{d}y, \tag{22}$$

or as the limit of a continuous product

$$\delta_\alpha(x) = \lim_{N\to\infty}\frac{\alpha}{\pi}\prod_{k=1}^{N}\cos\left(\frac{\alpha}{2^k}\,x\right) = \lim_{N\to\infty}\frac{1}{2^N\pi}\,\frac{\sin(\alpha x)}{\sin(\alpha/2^N x)}. \tag{23}$$

Numerically, Shannon's delta sequence kernel is one of the most important cases, because of its property of being an element of the Paley–Wiener reproducing kernel Hilbert space $B_{1/2}^2$

$$f(x) = \int_{-\infty}^{\infty} f(y)\,\frac{\sin[\pi(x-y)]}{\pi(x-y)}\,\mathrm{d}y \quad \forall f\in B_{1/2}^2, \tag{24}$$

where $\forall f\in B_{1/2}^2$ indicates that, in its Fourier representation, the L^2 function f vanishes outside the interval $[-\frac{1}{2},\frac{1}{2}]$. The Paley–Wiener reproducing kernel Hilbert space $B_{1/2}^2$ is a subspace of the Hilbert space $L^2(R)$.

Shannon's delta sequence kernel is also known as a wavelet scaling function $\phi(x) = \delta_\pi(x)$ [34, 35]. Shannon's mother wavelet can be constructed from the scaling function as

$$\psi(x) = \frac{\sin 2\pi x - \sin \pi x}{\pi x} \tag{25}$$

with its Fourier expression

$$\hat{\psi}(\omega) = \chi_{[-1,1]}(\omega) - \chi_{[-1/2,1/2]}(\omega). \tag{26}$$

This is recognized as the ideal band pass filter and it satisfies the orthonormality conditions

$$\sum_{n=-\infty}^{\infty}\hat{\psi}(\omega+n) = 1 \tag{27}$$

and

$$\sum_{n=-\infty}^{\infty}|\hat{\psi}(\omega+n)|^2 = 1. \tag{28}$$

Technically, it can be shown that a system of orthogonal wavelets are generated from a single function, the "mother" wavelet ψ, by standard operations of translation and dilation

$$\psi_{mn}(x) = 2^{-m/2}\,\psi\left(\frac{x}{2^m} - n\right), \quad m, n\in Z. \tag{29}$$

Shannon's delta sequence kernel can be derived from the generalized Lagrange interpolation formula

$$S_k(x) = \frac{G(x)}{G'(x_k)(x-x_k)}, \tag{30}$$

where $G(x)$ is an entire function given by

$$G(x) = (x - x_0) \prod_{k=1}^{\infty} \left(1 - \frac{x}{x_k}\right)\left(1 - \frac{x}{x_{-k}}\right) \tag{31}$$

and G' denotes the derivative of G. For a function band-limited to B, the generalized Lagrange interpolation formula $S_k(x)$ of equation (30) can provide an exact result

$$f(x) = \sum_{k \in Z} f(y_k)\, S_k(x), \tag{32}$$

whenever the set of non-uniform sampling points satisfy

$$\sup_{k \in Z} \left| x_k - \frac{k\pi}{B} \right| < \frac{\pi}{4B}, \tag{33}$$

where the symbol Z denotes the set of all integers. This is called the Paley and Wiener sampling theorem in the literature.

If $\{x_k\}_{k \in Z}$ are limited to a set of points on a uniform infinite grid ($x_k = k\Delta = -x_{-k}$), equation (31) can be simplified

$$G(x) = x \prod_{k=-\infty,\, k \neq 0}^{\infty} \left(1 - \frac{x}{k\Delta}\right) \tag{34}$$

$$= x \prod_{k=1}^{\infty} \left(1 - \frac{x^2}{k^2\Delta^2}\right) \tag{35}$$

$$= \Delta \frac{\sin(\pi/\Delta)\, x}{\pi}. \tag{36}$$

Since $G'(x_k)$ reduces to

$$G'(x_k) = (-1)^k \tag{37}$$

on a uniform grid, equation (30) gives rise to

$$S_k(x) = \frac{G(x)}{G'(x_k)(x - x_k)} = \frac{(-1)^k \sin(\pi/\Delta)\, x}{(\pi/\Delta)(x - k\Delta)} \tag{38}$$

$$= \frac{\sin(\pi/\Delta)(x - x_k)}{(\pi/\Delta)(x - x_k)}. \tag{39}$$

Obviously, $[\sin(\pi/\Delta)(x - x_k)]/(\pi/\Delta)(x - x_k)$ is an approximation to the delta distribution

$$\lim_{\Delta \to 0} \frac{\sin(\pi/\Delta)(x - x_k)}{(\pi/\Delta)(x - x_k)} \to \delta(x - x_k). \tag{40}$$

In fact, the generalized Lagrange interpolation formula directly gives rise to the delta distribution under an appropriate limit

$$\lim_{\max \Delta x \to 0} S_k(x) = \lim_{\max \Delta x \to 0} \frac{G(x)}{G'(x_k)(x - x_k)} \to \delta(x - x_k), \tag{41}$$

where max Δx is the largest Δx on the grid.

Both $\phi(x)$ and its associated wavelet play a crucial role in information theory and the theory of signal processing. However, their usefulness is limited by the fact that $\phi(x)$ and $\psi(x)$ are infinite impulse response (IIR) filters and their Fourier transforms $\hat{\phi}(\omega)$ and $\hat{\psi}(\omega)$ are not differentiable. From the computational point of view, $\phi(x)$ and $\psi(x)$ do not have finite moments in the co-ordinate space; in other words, they are delocalized.

According to the theory of distributions, the smoothness, regularity and localization of a temper distribution can be improved by a function of the Schwartz class. We apply this principle to regularize singular convolution kernels

$$\delta_{\sigma,\alpha}(x) = R_\sigma(x)\,\delta_\alpha(x) \quad (\sigma > 0), \tag{42}$$

where R_σ is a *regularizer* which has properties

$$\lim_{\sigma \to \infty} R_\sigma(x) = 1. \tag{43}$$

and

$$R_\sigma(0) = 1. \tag{44}$$

Here, equation (43) is a general condition that a regularizer must satisfy, while equation (44) is specifically for a *delta regularizer*, which is used in regularizing a delta kernel. Various delta regularizers can be used for numerical computations. A good example is the Gaussian

$$R_\sigma(x) = \exp\left[-\frac{x^2}{2\sigma^2} \right]. \tag{45}$$

The Gaussian regularizer is a Schwartz class function and has excellent numerical performance. However, we noted that in certain eigenvalue problems, no regularization is required if the potential is smooth and bounded from below (e.g., the harmonic oscillator potential $\frac{1}{2}x^2$).

For generality and simplicity, the following dimensionless parameters are introduced:

$$X = \frac{x}{a}, \qquad Y = \frac{y}{b}, \qquad W = \frac{w}{a}; \qquad \lambda = \frac{a}{b}; \qquad \sqrt{\frac{\rho h}{D}}. \tag{46}$$

Accordingly, we obtain the dimensionless governing equation for the vibration analysis of a rectangular plate as

$$\frac{\partial^4 W}{\partial X^4} + 2\lambda^2 \frac{\partial^4 W}{\partial X^2 \partial Y^2} + \lambda^4 \frac{\partial^4 W}{\partial Y^4} = \Omega^2 W. \tag{47}$$

Consider a uniform grid having

$$0 = X_0 < X_1 < \cdots < X_{N_x} = 1 \tag{48}$$

and

$$0 = Y_0 < Y_1 < \cdots < Y_{N_Y} = 1. \tag{49}$$

To formulate the eigenvalue problem, we introduce a column vector $\mathbf{W}$ as

$$\mathbf{W} = (W_{0,0}, \ldots, W_{0,N_Y}, W_{1,0}, \ldots, W_{N_X,N_Y})^{\mathrm{T}}, \tag{50}$$

with $(N_X + 1)(N_Y + 1)$ entries $W_{i,j} = W(X_i, Y_j)$, $(i = 0, 1, \ldots, N_X; j = 0, 1, \ldots, N_Y)$.

Let us define the $(N_q + 1) \times (N_q + 1)$ differentiation matrices $\mathbf{D}_q^n$ $(q = X, Y; n = 1, 2, \ldots)$, with their elements given by

$$[\mathbf{D}_q^n]_{i,j} = \delta_{\sigma,\Delta}^{(n)}(q_i - q_j), \quad (i, j = 0, \ldots, N_q), \tag{51}$$

where $\delta_{\sigma,\Delta}(q_i - q_j)$ is a DSC kernel of delta type [14]. Here, Δ is the grid spacing and σ determines the effective computational bandwidth. Many DSC kernels were constructed in the original work. Here, we choose a simple example, the regularized Shannon's delta kernel $\delta_{\sigma,\Delta}(q - q_j) = \sin[(\pi/\Delta)(q - q_j)]/[(\pi/\Delta)(q - q_j)]\, \mathrm{e}^{-(q-q_j)^2/(2\sigma^2)}$, to illustrate the algorithm and its application. Other DSC kernels, such as the regularized Dirichlet kernel and regularized Lagrange kernel, can also be used. The performance of a few DSC kernels for fluid dynamic computations and structural analysis was compared in reference [24]. As mentioned already, the differentiation in equation (51) can be *analytically* carried out

$$\delta_{\sigma,\Delta}^{(n)}(q_i - q_j) = \left[\left(\frac{\mathrm{d}}{\mathrm{d}q}\right)^n \delta_{\sigma,\Delta}(q - q_j)\right]_{q=q_i} = C_m^n, \tag{52}$$

where, for a uniform grid spacing, $m = (q_i - q_j)/\Delta$. Here, the matrix is banded to $i - j = m = -M, \ldots, 0, \ldots, M$. Therefore, the system of linear algebraic equations for the governing PDE (47) is given by

$$(\mathbf{D}_X^4 \otimes \mathbf{I}_Y + 2\lambda^2 \mathbf{D}_X^2 \otimes \mathbf{D}_Y^2 + \lambda^4 \mathbf{I}_X \otimes \mathbf{D}_Y^4)\, \mathbf{W} = \Omega^2 \mathbf{W}, \tag{53}$$

where $\mathbf{I}_q$ is the $(N_q + 1)^2$ unit matrix and $\otimes$ denotes the tensorial product. Eigenvalues can be evaluated from equation (53) by using a standard solver. However, appropriate boundary conditions are to be implemented before calculating eigenvalues. This is described below.

We first note that boundary condition $W = 0$ is easily specified at the edge. To implement other boundary conditions, we assume, for a function f, the following relation between the inner and outer nodes on the left boundary

$$f(X_{-m}) - f(X_0) = \left(\sum_{j=0}^{J} a_m^j X_m^j\right)[(f(X_m) - f(X_0)], \tag{54}$$

where coefficients a_m^j $(m = 1, \ldots, M, j = 0, 1, \ldots J)$ are to be determined by the boundary conditions. For the three types of boundary conditions described earlier, we only need to consider the zeroth order term in the power of X^j. Therefore, we set $a_m^0 \equiv a_m$ and, after

rearrangement, obtain

$$f(X_{-m}) = a_m f(X_m) + (1 - a_m) f(X_0), \quad m = 1, 2, \ldots, M. \tag{55}$$

According to equation (52), the first and second derivatives of f on the boundary are approximated by

$$f'(X_0) = \sum_{m=-M}^{M} C_m^1 f(X_m) \tag{56}$$

$$= \left[C_0^1 - \sum_{m=1}^{M} (1 - a_m)\, C_m^1 \right] f(X_0) + \sum_{m=1}^{M} (1 - a_m)\, C_m^1 f(X_m) \tag{57}$$

and

$$f''(X_0) = \sum_{m=-M}^{M} C_m^2 f(X_m)$$

$$= \left[C_0^2 + \sum_{m=1}^{M} (1 - a_m)\, C_m^2 \right] f(X_0) + \sum_{m=1}^{M} (1 - a_m)\, C_m^2 f(X_m)$$

respectively.

For simply supported edges, the boundary conditions reduce to

$$f(X_0) = 0, \qquad f''(X_0) = 0. \tag{58}$$

These are satisfied by choosing $a_m = -1, m = 1, 2, \ldots, M$. This is the so-called *anti-symmetric extension* [14].

For clamped edges, the boundary conditions require

$$f(X_0) = 0, \qquad f'(X_0) = 0. \tag{59}$$

These are satisfied by $a_m = 1, m = 1, 2, \ldots, M$. This is the *symmetric extension* [14].

Expressions for the right, top and bottom boundaries can be derived in a similar way.

In view of possible presence of irregular internal support condition, matrices $\mathbf{D}_X^4$, $\mathbf{D}_Y^4$, $\mathbf{D}_X^2$, $\mathbf{D}_Y^2$, $\mathbf{I}_X$ and $\mathbf{I}_Y$ become three-dimensional ones in this work and are denoted by $\mathscr{D}_X^4$, $\mathscr{D}_Y^4$, $\mathscr{D}_X^2$, $\mathscr{D}_Y^2$, $\mathscr{I}_X$ and $\mathscr{I}_Y$. The matrix elements of $\mathscr{D}_X^p$, $(p = 2, 4)$ are denoted by $d_{X,ijk}^p$, $(i, j = 0, 1, 2, \ldots, N_X; k = 0, 1, 2, \ldots, N_Y)$ and matrix elements of $\mathscr{I}_X$ are denoted by $\delta_{ij} \otimes 1_k$, $(k = 0, 1, 2, \ldots, N_Y)$. $\mathscr{D}_Y^p$ and $\mathscr{I}_Y$ are similarly defined by appropriately switching the roles of the subscripts.

Let us define a contractive tensor product $\dot{\otimes}$ of two three-dimensional matrices $\mathscr{A}$ and $\mathscr{B}$ as the tensor product on the first two indices of $\mathscr{A}$ and $\mathscr{B}$, and contraction between the first and third indices of the two matrices

$$(\mathscr{A} \dot{\otimes} \mathscr{B})_{i \times N_y + k,\ j \times N_y + l} = a_{ijk} b_{kli}, \tag{60}$$

where a_{ijk} and b_{kli} are matrix elements of $\mathscr{A}$ and $\mathscr{B}$ respectively. In such a notation, equation (53) is modified as

$$(\mathscr{D}_X^4 \dot{\otimes} \mathscr{I}_Y + 2\lambda^2 \mathscr{D}_X^2 \dot{\otimes} \mathscr{D}_Y^2 + \lambda^4 \mathscr{I}_Y \dot{\otimes} \mathscr{D}_Y^4)\, \mathbf{W} = \Omega^2 \mathbf{W}, \tag{61}$$

where the lexicographic ordering given in equation (60) is used for reducing four-dimensional matrices into two-dimensional forms. Matrix elements in equation (61)

are ready for being used in a linear equation solver

$$\mathscr{I}_X \dot{\otimes} \mathscr{D}_Y^4 = \left(\begin{array}{ccc|cc|c} d_{Y,000}^4 & d_{Y,010}^4 & \cdots & & & \\ d_{Y,100}^4 & d_{Y,110}^4 & \cdots & \multicolumn{2}{c|}{\vdots\ \vdots\ \ddots} & \cdots \\ \vdots & \vdots & \ddots & & & \\ \hline & & & d_{Y,001}^4 & d_{Y,011}^4 \quad \cdots & \\ \multicolumn{2}{c|}{\vdots\ \vdots\ \ddots} & & d_{Y,101}^4 & d_{Y,111}^4 \quad \cdots & \cdots \\ & & & \vdots & \vdots \quad \ddots & \\ \hline \multicolumn{2}{c|}{\vdots} & & \multicolumn{2}{c|}{\vdots} & \ddots \end{array}\right),$$

$$\mathscr{D}_X^4 \dot{\otimes} \mathscr{I}_Y = \left(\begin{array}{cccc|cccc|c} d_{X,000}^4 & 0 & \cdots & 0 & d_{X,010}^4 & 0 & \cdots & 0 & \\ 0 & d_{X,001}^4 & \cdots & 0 & 0 & d_{X,011}^4 & \cdots & 0 & \\ \vdots & & \ddots & \vdots & \vdots & & \ddots & \vdots & \cdots \\ 0 & \cdots & \cdots & d_{X,00N_Y}^4 & 0 & \cdots & \cdots & d_{X,01N_Y}^4 & \\ \hline d_{X,100}^4 & 0 & \cdots & 0 & d_{X,110}^4 & 0 & \cdots & 0 & \\ 0 & d_{X,101}^4 & \cdots & 0 & 0 & d_{X,111}^4 & \cdots & 0 & \\ \vdots & & \ddots & \vdots & \vdots & & \ddots & \vdots & \cdots \\ 0 & \cdots & \cdots & d_{X,10N_Y}^4 & 0 & \cdots & \cdots & d_{X,11N_Y}^4 & \\ \hline & & \vdots & & & & \vdots & & \ddots \end{array}\right)$$

and

$$\mathscr{D}_x^2 \dot{\otimes} \mathscr{D}_y^2 = \left(\begin{array}{ccc|ccc|c} d_{X,000}^2 d_{Y,000}^2 & d_{X,000}^2 d_{Y,010}^2 & \cdots & d_{X,010}^2 d_{Y,000}^2 & d_{X,010}^2 d_{Y,010}^2 & \cdots & \\ d_{X,001}^2 d_{Y,100}^2 & d_{X,001}^2 d_{Y,110}^2 & \cdots & d_{X,011}^2 d_{Y,100}^2 & d_{X,011}^2 d_{Y,110}^2 & \cdots & \cdots \\ \vdots & \vdots & \ddots & \vdots & \vdots & \ddots & \\ \hline d_{X,100}^2 d_{Y,001}^2 & d_{X,100}^2 d_{Y,011}^2 & \cdots & d_{X,110}^2 d_{Y,001}^2 & d_{X,110}^2 d_{Y,011}^2 & \cdots & \\ d_{X,101}^2 d_{Y,101}^2 & d_{X,101}^2 d_{Y,111}^2 & \cdots & d_{X,111}^2 d_{Y,101}^2 & d_{X,111}^2 d_{Y,111}^2 & \cdots & \cdots \\ \vdots & \vdots & \ddots & \vdots & \vdots & \ddots & \\ \hline & \vdots & & & \vdots & & \ddots \end{array}\right).$$

An internal line support in a plate is modelled as a series of point supports along the line support. Assume that the set of internal support points are given by $\{(X_{i'}, Y_{j'})\}$, the internal support conditions ($W_{i,j} = 0, \forall (X_i, Y_j) \in \{(X_{i'}, Y_{j'})\}$) are specified pointwisely in the matrix construction.

2.3. THE LEVY METHOD

An analytical approach based on the Levy method was developed by the authors to obtain the exact solutions for the vibration of rectangular plates with internal line supports [36]. The solution procedure is briefly summarized herein.

We consider that a rectangular plate consists of n spans that are divided at the locations of the $(n-1)$ internal line supports (see Figure 3). These internal line supports impose zero

deflection constraint along the line supports in the plate. The governing differential equation for free vibration of the ith span is given by

$$\frac{\partial^4 w_i}{\partial x^4} + 2\frac{\partial^4 w_i}{\partial x^2 \partial y^2} + \frac{\partial^4 w_i}{\partial y^4} = \frac{\rho h \omega^2}{D} w_i \tag{62}$$

in which the subscript i ($= 1, 2, \ldots, n$) refers to the ith span in the plate and $w_i(x, y)$ is the transverse displacement.

Along the interface between the ith and $(i + 1)$th spans, the following essential and natural boundary conditions must hold to ensure the continuity of the plate and the satisfaction of the internal line support condition [36]:

$$w_i = 0, \tag{63}$$

$$w_{i+1} = 0, \tag{64}$$

$$\frac{\partial w_i}{\partial x} = \frac{\partial w_{i+1}}{\partial x}, \tag{65}$$

$$\frac{\partial^2 w_i}{\partial x^2} + \nu \frac{\partial^2 w_i}{\partial y^2} = \frac{\partial^2 w_{i+1}}{\partial x^2} + \nu \frac{\partial^2 w_{i+1}}{\partial y^2}. \tag{66}$$

Assume that the plate is simply supported on the two edges parallel to the x-axis. For such a rectangular plate, we may use the Levy method for solution. The displacement function for the ith span can be expressed as

$$w_i(x, y) = \sin\left(\frac{m\pi}{L} y\right) X_i(x), \quad i = 1, 2, \ldots, n, \tag{67}$$

where m is the number of half-waves of the vibration mode in the y direction. Equation (67) satisfies the boundary conditions for the two simply supported edges parallel to the x-axis.

In view of equations (67) and (62), a homogeneous differential equation system for the ith span can be derived as follows:

$$\mathbf{\Psi}_i' - \mathbf{H}_i \mathbf{\Psi}_i = 0, \quad i = 1, 2, \ldots, n \tag{68}$$

in which

$$\mathbf{\Psi}_i = \begin{Bmatrix} X_i \\ X_i' \\ X_i'' \\ X_i''' \end{Bmatrix} \tag{69}$$

and the prime denotes differentiation with respect to x; $\mathbf{\Psi}_i'$ is the first derivative of $\mathbf{\Psi}_i$; and $\mathbf{H}_i$ is a 4×4 matrix with identical elements for each span. The non-zero elements of $\mathbf{H}_i$ are given by

$$H_{12} = H_{23} = H_{34} = 1, \tag{70}$$

$$H_{41} = \frac{\rho h \omega^2}{D} - \left(\frac{m\pi}{L}\right)^4, \tag{71}$$

$$H_{43} = 2\left(\frac{m\pi}{L}\right)^2. \tag{72}$$

The procedure for solving equation (68) has been detailed by Xiang *et al.* [5]. The solution for equation (68) can be expressed as

$$\mathbf{\Psi}_i = \mathbf{e}^{\mathbf{H}_i x}\mathbf{c}_i, \tag{73}$$

in which $\mathbf{e}^{\mathbf{H}_i x}$ is a general matrix solution for equation (68); $\mathbf{c}_i$ is a 4×1 constant column matrix that will be determined by the plate boundary conditions and/or span interface conditions.

In view of equation (73), a homogeneous system of equations can be derived by implementing the boundary conditions of the plate along the two edges parallel to the y-axis and the interface conditions between two spans, equations (63)–(66), when assembling the spans to the whole plate

$$\mathbf{K}\begin{Bmatrix} \mathbf{c}_1 \\ \mathbf{c}_2 \\ \vdots \\ \mathbf{c}_i \\ \mathbf{c}_{i+1} \\ \vdots \\ \mathbf{c}_n \end{Bmatrix} = \{\mathbf{0}\}, \tag{74}$$

where $\mathbf{K}$ is a $4n \times 4n$ matrix. The vibration frequency ω is evaluated by setting the determinant of $\mathbf{K}$ to zero.

3. RESULTS AND DISCUSSION

The application of the DSC algorithm to the analysis of high-frequency vibrations is demonstrated in this section. Extensive numerical studies are carried out for the vibration analysis of beam and two-span plates. The detailed studies of these two problems are presented in the following two subsections.

3.1. NUMERICAL STUDY OF THE BEAM

The beam problem described by equations (5) and (6) is considered in this subsection. For such a beam, one of the present authors (GWW) studied [26] the DSC performance for the first 10 eigenvalues. The purpose of the present study is to examine the DSC behavior for higher order modes. For simplicity, we exclude force term $S = 0$ and choose a computational domain of $[0, 100\pi]$. Thus, exact eigenvalues (8) are given by

$$\left(\frac{n}{100}\right)^4. \tag{75}$$

The reliability and accuracy of the DSC algorithm for this problem are tested by convergence study and error analysis respectively.

TABLE 1

Convergence and comparison of the frequency parameters for an SS beam

Mode number	Mesh size										Analytical solution
	1001	2001	3001	4001	5001	6001	7001	8001	9001	10 001	
500	25·0002	25·0000	25·0000	25·0000	25·0000	25·0000	25·0000	25·0000	25·0000	25·0000	25·0000
1000	—	100·0010	100·0000	100·0000	100·0000	100·0000	100·0000	100·0000	100·0000	100·0000	100·0000
2000	—	—	401·2058	400·0040	400·0000	400·0000	400·0000	400·0000	400·0000	400·0000	400·0000
3000	—	—	—	917·8974	900·3730	900·0090	900·0004	900·0000	900·0000	900·0000	900·0000
4000	—	—	—	—	1670·5393	1604·8234	1600·2503	1600·0160	1600·0014	1600·0002	1600·0000
5000	—	—	—	—	—	2661·4351	2524·0720	2502·2878	2500·2205	2500·0250	2500·0000
6000	—	—	—	—	—	—	3882·4488	3671·5896	3610·8526	3601·4920	3600·0000
7000	—	—	—	—	—	—	—	5324·9235	5056·6271	4934·0755	4900·0000

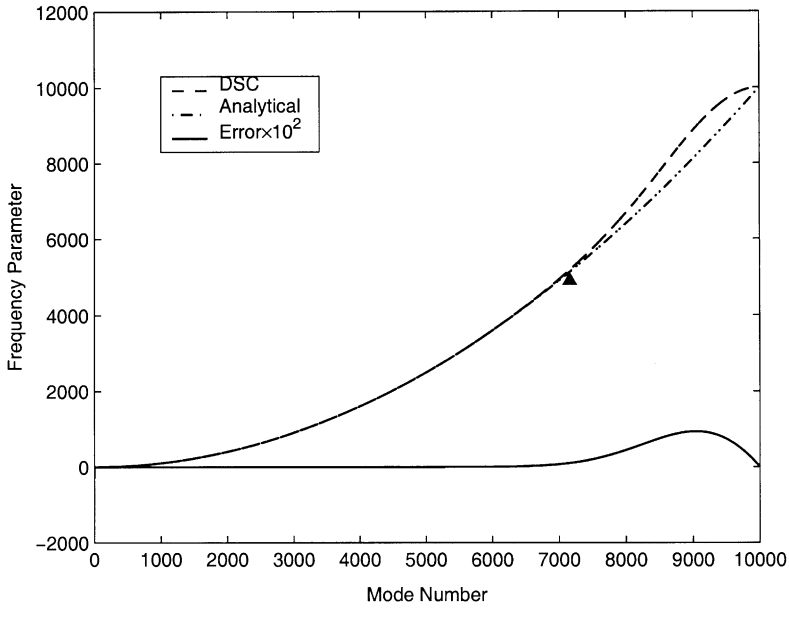

Figure 1. Comparison of frequency parameters between DSC and analytical solutions to an SS beam (including absolute errors).

3.1.1 *Convergence study*

The speed of the convergence of a numerical method is an important character for a given problem. To examine the convergence of the DSC algorithm for the beam analysis, only the 500th mode and higher order modes are considered in the present study, as lower order modes were studied in reference [26]. We use a set of uniform grids of 1001, 2001, 3001, $\cdots$, 10 001 points to test the speed of the convergence of the DSC algorithm. The DSC results are listed in Table 1. When the DSC grid is 1001, the first 500 modes are firmly converged. Such a result is consistent with the previous study [26], where 15 significant-figure accuracy was achieved for the first 10 eigenvalues by using both the regularized Shannon kernel and the regularized Dirichlet kernel with a grid of 32 points. At the grid of 2001, the first 1000 modes have converged to five significant figures. Similarly, the first 2000 modes have converged to five significant figures at the grid of 4001. This pattern can be tracked to the 4000th mode, i.e., its accuracy of five significant figures is reached at the grid of 8001 points. We also find that the same accuracy is achieved for the first 5000 modes at the grid of 10 001 points. It is reasonable to extrapolate that this excellent accuracy will be attained for the 10 000th mode at the grid of 20 001 points. It is also found that when the number of grid points is 10 001, the 6000th mode has already converged to 1·5 in 3600 parts. Obviously, the DSC results are remarkable and the best ever attained for this problem.

3.1.2. *Error analysis*

Error analysis is performed to further validate the DSC algorithm for high-frequency vibration analysis. The DSC calculation is conducted for $N = 10\,001$ grid points. Both the analytical and the DSC results are plotted in Figure 1 for the first 10 000 eigenmodes. We also present in Figure 1 the relative errors for each eigenmode. The relative errors E_{re} are assessed as

$$E_{re} = \frac{|f_{exact} - f_{num}|}{f_{exact}} \times 100\%,$$

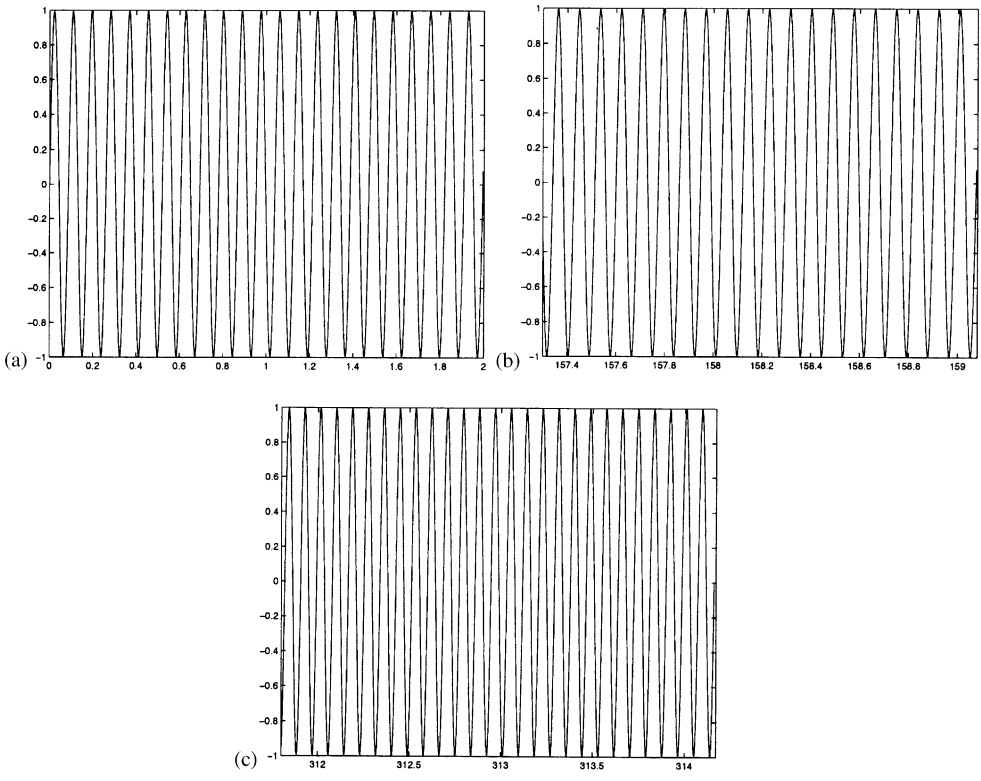

Figure 2. Plot of portions of the 7250th mode shape of an SS beam of length 100π: (a) at the left end; (b) in the center and (c) at the right end.

where f_{exact} and f_{num} are exact and numerical eigenvalues respectively. When using 10 001 DSC grid points, it is found that the relative error for mode 1000 is $8E(-11)\%$. The smallest error is $<1E(-16)\%$ which occurs at mode 1585. The relative error at mode 1700 is $1{\cdot}8E(-11)\%$. After mode 1700, the relative errors increase essentially monotonically to $1{\cdot}4E(-10)$, $5{\cdot}0E(-8)$, $1{\cdot}0E(-5)$, $1{\cdot}0E(-3)$, $4{\cdot}1E(-2)$ and $6{\cdot}9E(-1)\%$ at modes 2000, 3000, 4000, 5000, 6000 and 7000, respectively. In fact, all relative errors are below 1 and 2% for the first 7161 modes and 7500 modes respectively. We found that the largest error is $<9{\cdot}3\%$ and it occurs around mode 9000. It is interesting to note that the relative errors decrease gradually after mode 9000 and reduce to $<2E(-2)\%$ for the mode 9999. Numerically, it takes *at least* three grid points to support a single half-wave and *at least* five grid points to support two half-waves. However, when the number of grid points is very large, the Nyquist limit gives a ratio of one grid point per half-wave. In practical computations, such a limit can never been achieved. If the error is controlled within 1%, the present DSC algorithm achieves the ratio of 1·4 grid points per half-wave. Such a high ratio has not been reported in the vibration literature to our knowledge.

Since the eigenvalues given by equation (75) are densely distributed, it is possible that the relative errors of the numerical results are not too large, while the corresponding eigenfunctions are mismatched. To find out where such mismatches first occur, we have examined detailed mode shapes. It is found that no mismatch occurs for the first 7250 modes. The eigenfunction of mode 7250 is depicted in Figure 2. The number of half-waves is the same as the mode number and there is no distortion in the mode shape.

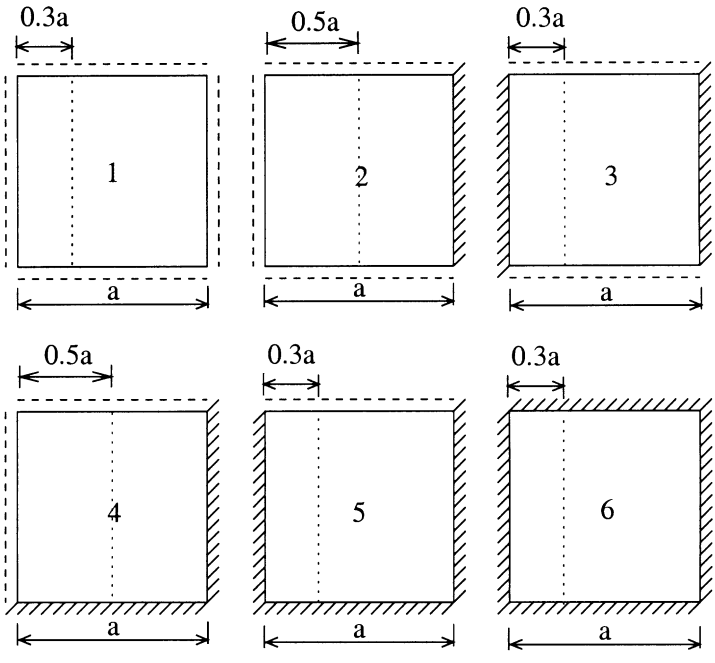

Figure 3. Square plates with six combinations of edge support conditions and an internal line support.

3.2. NUMERICAL RESULTS FOR TWO-SPAN PLATES

The DSC algorithm is applied to the high-frequency vibration analysis of plates with internal line supports in this subsection. Figure 3 depicts square plates with six distinct boundary conditions and corresponding internal support positions. The boundary conditions are obtained by a combination of simply supported and clamped edges. The Poisson ratio is taken as 0·3 when needed. The DSC algorithm is used to compute the eigenvalues for all the six cases. All the frequency parameters are reported as Ω/π^2 with the Ω being defined in equation (46). The Levy solution, which can be arbitrarily accurate, is also employed to provide a cross validation of the DSC algorithm. The Levy approach is readily available for Cases 1–3, to give exact solutions as long as the internal line supports are normal to the two simply supported parallel edges. In fact, Case 1 without internal support (i.e., a four-edge simply supported square plate) is analytically solvable and its non-trivial frequency parameters are explicitly given by

$$\frac{\Omega_{n_x,n_y}}{\pi^2} = n_x^2 + n_y^2 \quad (n_x, n_y = 1, 2, \ldots),$$

where n_x and n_y are the number of halfwaves of the solution in the x and y directions respectively. To test the reliability of the present Levy code, the complete set of the first 7755 modes for a four-edge simply supported square plate has been computed against the analytical solution. It is found that our Levy results are indeed reliable and arbitrarily accurate.

3.2.1 *Convergence studies*

Having built up our confidence with the DSC approach for the high-frequency vibration analysis of the beam, it is necessary to further test the reliability level of the DSC

TABLE 2

Convergence and comparison of the frequency parameters for an SSCS plate with a central line support, Case 2

Mode number	Mesh size										Levy's solution
	11^2	21^2	31^2	41^2	51^2	61^2	71^2	81^2	91^2	101^2	
1	5·5907	5·5813	5·5809	5·5808	5·5808	5·5808	5·5808	5·5808	5·5808	5·5808	5·5808
10	22·0807	21·7935	21·7801	21·7770	21·7760	21·7755	21·7753	21·7752	21·7751	21·7751	21·7749
50	94·8264	83·3298	83·1939	83·1604	83·1492	83·1441	83·1441	83·1399	83·1390	83·1384	83·1368
100	—	158·3874	156·9748	156·8918	156·8676	156·8570	156·8515	156·8485	156·8466	156·8455	156·8423
300	—	488·9399	433·9706	431·7785	431·5771	431·4949	431·4537	431·4307	431·4168	431·4079	431·3839
500	—	—	748·6920	696·4816	694·1659	693·9051	693·7906	693·7282	693·6907	693·6670	693·6034
700	—	—	1071·1865	981·6820	965·9805	965·2393	965·2164	965·2127	965·2107	965·2094	965·2055
1000	—	—	—	1434·9975	1369·6018	1363·5763	1362·3769	1361·5607	1361·0717	1360·7578	1360·5185
1500	—	—	—	—	2116·9111	2031·4074	2024·0763	2021·7201	2021·6462	2020·8887	2018·8270
2000	—	—	—	—	2887·7529	2764·8757	2683·1905	2673·2309	2669·3727	2669·2634	2668·3420
2500	—	—	—	—	—	3502·8247	3405·8533	3332·6415	3320·0799	3317·1609	3315·0637
3000	—	—	—	—	—	4386·9027	4163·6380	4025·1308	3985·9518	3970·7934	3967·0804
3500	—	—	—	—	—	—	4861·9311	4767·3490	4661·2424	4630·0394	4626·5807
4000	—	—	—	—	—	—	5691·6385	5533·6553	5369·2213	5290·4119	5269·7221
4500	—	—	—	—	—	—	7570·9766	6237·6232	6106·0312	5975·6228	5916·7632
5000	—	—	—	—	—	—	—	6911·2309	6870·5240	6692·5416	6562·5454

TABLE 3

Convergence and comparison of the frequency parameters for a CCCS plate with a line support at three-tenth of the edge, Case 5

Mode number	Mesh size										Analytical solution
	11^2	21^2	31^2	41^2	51^2	61^2	71^2	81^2	91^2	101^2	
1	4·9370	4·9097	4·9084	4·9081	4·9081	4·9080	4·9080	4·9080	4·9080	4·9080	NA
10	28·0142	25·9506	25·9025	25·8921	25·8889	25·8875	25·8868	25·8864	25·8861	25·8860	NA
50	100·4648	88·3117	88·0676	87·9526	87·9100	87·8909	87·8812	87·8757	87·8723	87·8702	NA
100	—	162·8809	161·0435	160·7151	160·6188	160·5761	160·5543	160·5420	160·5346	160·5299	NA
300	—	508·8399	449·2018	444·3581	443·8152	443·4535	443·3484	443·2899	443·2546	443·2319	NA
500	—	—	767·4629	711·2141	708·6403	708·3103	708·1602	708·0771	708·0270	707·9949	NA
700	—	—	1086·7947	999·0392	985·1239	983·5381	982·3237	981·6934	981·3203	981·0835	NA
1000	—	—	—	1458·2970	1389·0084	1383·5202	1382·2355	1381·6627	1381·3015	1381·0624	NA
1500	—	—	—	—	2150·9475	2064·8612	2045·0983	2041·5426	2040·0409	2039·2387	NA
2000	—	—	—	—	2911·9239	2807·0083	2719·0551	2702·5745	2700·8542	2699·8622	NA
2500	—	—	—	—	—	3531·5203	3443·5612	3369·7486	3355·8767	3353·1464	NA
3000	—	—	—	—	—	4425·8219	4211·1010	4064·8111	4018·2753	4008·7738	NA
3500	—	—	—	—	—	—	4892·5179	4815·3400	4700·6282	4673·6958	NA
4000	—	—	—	—	—	—	5728·1643	5585·1467	5419·0211	5333·6821	NA
4500	—	—	—	—	—	—	7625·9013	6281·5808	6167·4912	6022·2732	NA
5000	—	—	—	—	—	—	—	6958·5537	6933·2539	6750·0937	NA

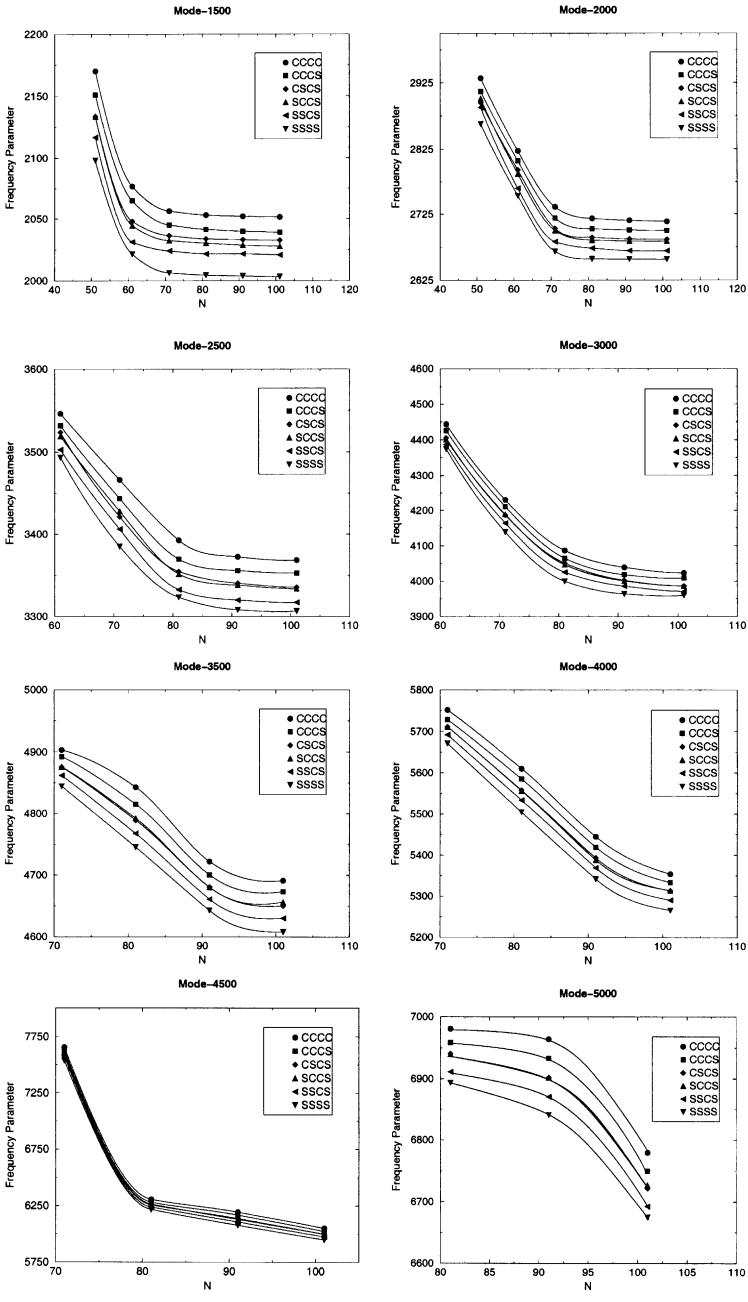

Figure 4. Convergence study of frequency parameters for plates with internal line supports (Modes 1, 10, 50, 100, 300, 500, 700, 1000, 1500, 2000, 2500, 3000, 3500, 4000, 4500, 5000).

high-frequency prediction for plates. To verify the validity and accuracy of the proposed DSC approach, convergence and comparison studies are carried out for all the six cases. In particular, more detailed results are given for Cases 2 and 5. Here, Case 2 admits the Levy exact solution, and thus provides another objective test for the proposed DSC approach. It is also important to examine the behavior of the DSC algorithm for a class of real vibration

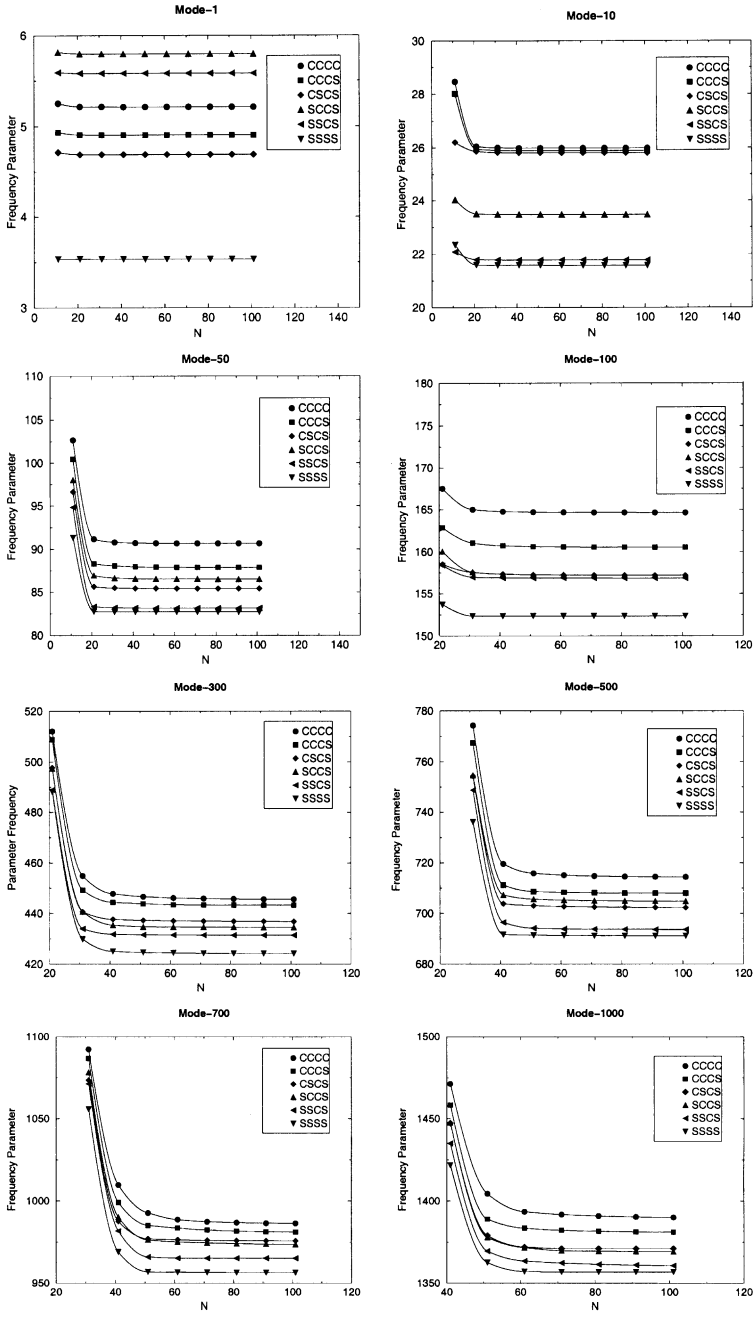

Figure 4. Continued

problems that are not analytically solvable. Therefore, Case 5 is selected for the detailed convergence studies.

We conduct the convergence studies for all the six cases with a number of DSC grids, ranging from 11^2 points to 101^2 points. The speed of convergence for the first 5000 modes has been checked. These results are presented in Tables 2 and 3 for Cases 2 and 5 respectively. Obviously, these DSC results converge to the Levy exact solution for Case 2. It

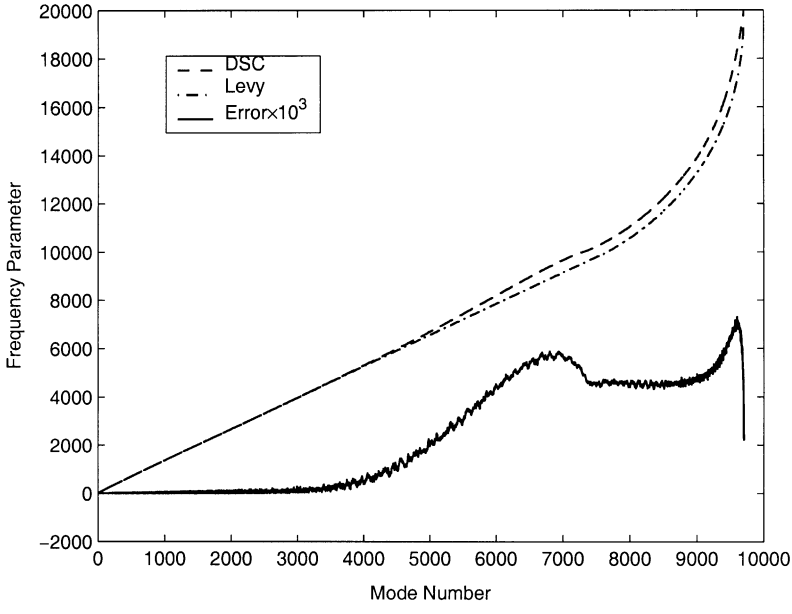

Figure 5. Comparison of frequency parameters between DSC and Levy solutions to an SSCS plate with internal line supports, Case 2 (including absolute errors).

is seen from Table 2 that the first 100 modes have converged at the grid of 31^2 points. The degree of convergence in these modes is not as firm as that in the beam for the same level of computations, because the inherent complexity in the plate problem. Nevertheless, we note that the first 500 modes converge to much less than 0·1% relative errors at the grid of 51^2 points and the first 1000 modes with relative errors $<0{\cdot}3\%$ at the grid of 61^2 points. At the DSC grid of 81^2 points, the relative errors of the first 2000 modes are $<0{\cdot}2\%$. In fact, at the final grid of 101^2 points, the relative errors of first 2500 modes and 3000 modes are less than 0·07 and 0·1% respectively. Remarkably, the relative errors for the first 4000, 4500, and 5000 modes are less than 0·4, 1 and 2%, respectively, on this grid. It is noted that the maximum relative error is $<6\%$ for all modes to the left of mode 7755. Such a result indicates that the solution of the DSC algorithm is very reliable for the first 40% modes computed and is quite reliable for the modes filling between the first 40–50% (within 2% errors). The DSC results become less reliable, but are still useful for the modes filling between the first 50–75%. Although the last 25% modes are unreliable for being used quantitatively, however, the tendency of the DSC results for that section is still reasonable.

The detailed convergence study for Case 5 is listed in Table 3. The convergence pattern of Case 5 is almost identical to that of Case 2. This can be easily confirmed by a comparison of the speed of convergence in Tables 2 and 3. Such a great similarity between the results of Cases 2 and 5 indicates that the convergence of the DSC algorithm is not sensitive to different boundary and support conditions.

A comprehensive comparison of the convergence pattern for all the six cases is plotted in Figure 4. A large set of modes, i.e., modes 1, 10, 50, 100, 300, 500, 700, 1000, 1500, 2000, 2500, 3000, 3500, 4000, 4500, and 5000, are examined. Appropriate numbers of grid points used for this comparison are $11^2, 21^2, \ldots, 101^2$. The first mode of each case is essentially converged at the grid of 11^2 points. Similarly, the first 50 modes of each case are firmly converged at the grid of 21^2 points. The first 500 modes show a good convergence at the grid of 41^2 points. Very firm convergence is also observed for the first 2000 modes of all the

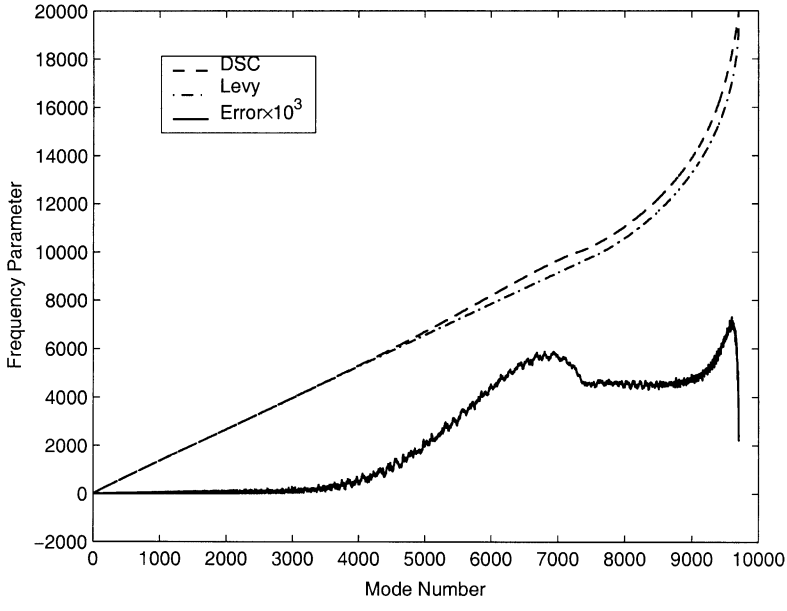

Figure 6. Comparison of frequency parameters between DSC and Levy solutions to an SSSS plate with internal line supports, Case 1 (including absolute errors).

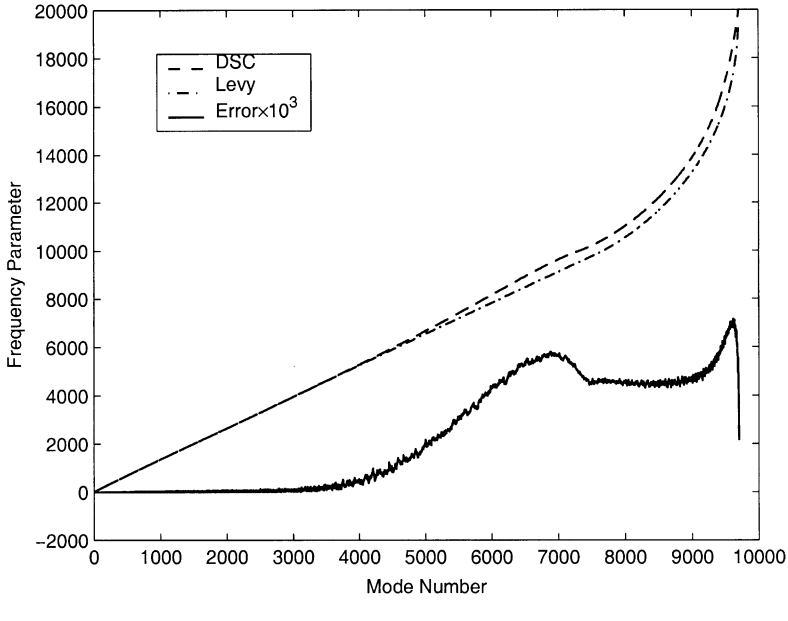

Figure 7. Comparison of frequency parameters between DSC and Levy solutions to a CSCS plate with internal line supports, Case 3 (including absolute errors).

six cases. In general, higher order modes converge slowly at a given set of grid points because they require a larger number of grid points to reach the convergence. Obviously, the mode 5000 of each case has not converged. Typical relative errors for such mode at the grid of 101^2 points are about 2% in the present computation. It is important to see from

TABLE 4

Benchmark solutions for a wide range of frequency parameters for SCCS, CCCS, CCCC, SSSS, SSCS and CSCS plates with internal line support (m is the number of half-waves in the y direction and n is the number of half-waves in the x direction)

Mode number	SCCS	CCCS	CCCC	SSSS			SSCS			CSCS		
				m, *n*	Levy	DSC	*m*, *n*	Levy	DSC	*m*, *n*	Levy	DSC
1	5·7956	4·9080	5·2133	1, 2	3·5358	3·5358	1, 2	5·5808	5·5808	1, 2	4·6915	4·6915
2	8·8785	7·8999	8·7860	2, 2	6·3655	6·3655	2, 2	8·4352	8·4352	2, 2	7·1588	7·1588
3	9·1324	12·1929	12·3580	1, 3	9·6986	9·6986	1, 3	8·7318	8·7318	3, 2	11·8093	11·8093
4	11·5510	13·1295	14·5968	3, 2	11·2676	11·2676	2, 3	10·9914	10·9915	1, 3	12·0598	12·0599
5	14·5727	15·1608	15·7445	2, 3	12·6499	12·6499	3, 2	13·3265	13·3265	2, 3	14·6656	14·6656
6	16·4023	20·2353	20·6636	1, 4	14·9489	14·9490	3, 3	15·2887	15·2888	4, 2	18·6088	18·6089
7	18·4135	20·4863	21·3544	3, 3	17·5956	17·5956	1, 4	18·3022	18·3022	3, 3	19·2426	19·2427
8	21·5753	20·5498	22·5048	2, 4	17·6681	17·6682	4, 2	20·2556	20·2556	1, 4	20·4531	20·4533
9	22·0516	23·2340	23·6661	4, 2	18·2122	18·2122	2, 4	21·1577	21·1577	2, 4	22·8616	22·8619
10	23·4683	25·8860	25·9831	1, 5	21·5771	21·5772	4, 3	21·7749	21·7751	1, 5	25·8024	25·8029
11	24·2468	27·4307	28·7322	3, 4	22·3279	22·3280	1, 5	24·1575	24·1578	4, 3	25·8883	25·8885
12	26·8510	27·8394	28·8579	2, 5	24·3377	24·3379	3, 4	25·9952	25·9953	3, 4	27·0488	27·0492
13	26·9747	28·4807	29·1150	4, 3	24·5463	24·5463	2, 5	26·6275	26·6279	5, 2	27·4869	27·4870
14	31·5424	29·9023	32·4528	5, 2	27·1778	27·1778	5, 2	29·2084	29·2084	2, 5	28·1491	28·1495
15	31·6727	33·0584	33·8670	4, 4	29·0070	29·0072	5, 3	30·4213	30·4215	3, 5	32·3385	32·3391
16	32·6810	34·4815	35·9105	3, 5	29·0544	29·0546	3, 5	30·9270	30·9274	4, 4	33·1788	33·1794
17	34·2138	36·7170	38·9621	5, 3	33·5042	33·5042	4, 4	32·8504	32·8505	5, 3	34·6151	34·6152
18	38·4376	39·7779	40·1036	1, 6	35·2941	35·2942	4, 5	37·2052	37·2058	6, 2	38·4067	38·4068
19	39·0605	40·0236	41·0996	4, 5	35·7939	35·7941	1, 6	38·9854	38·9856	4, 5	38·5710	38·5716
20	42·1628	41·3481	43·2227	5, 4	37·7359	37·7362	6, 2	40·1752	40·1753	1, 6	39·9520	39·9526
22	43·6317	43·2291	45·2249	2, 6	38·2213	38·2214	5, 4	41·7319	41·7320	2, 6	42·6344	42·6350
24	47·3059	48·0651	50·5501	6, 3	44·4690	44·4691	5, 5	45·5490	45·5498	5, 5	46·9308	46·9316
26	47·6152	54·0991	55·8322	6, 4	48·5165	48·5168	1, 7	47·5502	47·5514	7, 2	51·3505	51·3506
28	54·5989	54·8105	57·2929	4, 6	50·0098	50·0099	6, 4	52·6372	52·6373	4, 6	53·7093	53·7103
30	55·1148	59·7227	60·4225	2, 7	51·9245	51·9247	4, 6	53·5573	53·5576	6, 5	57·4226	57·4235
32	57·3447	61·4496	64·7887	3, 7	56·8286	56·8288	3, 7	54·5534	54·5549	2, 7	59·9296	59·9307
34	61·8017	65·0904	65·6507	7, 3	57·4397	57·4397	4, 7	60·8603	60·8621	7, 4	64·0957	64·0971
36	67·7189	67·0928	68·8799	2, 8	59·9333	59·9345	7, 4	65·5616	65·5618	1, 8	65·9564	65·9596
38	70·5399	70·2827	72·9719	4, 7	63·7077	63·7080	8, 2	68·1324	68·1325	2, 8	68·4399	68·4434

TABLE 4

Continued

Mode number	SCCS	CCCS	CCCC	SSSS			SSCS			CSCS		
				m, *n*	Levy	DSC	*m*, *n*	Levy	DSC	*m*, *n*	Levy	DSC
40	71·4126	72·8826	74·3868	8, 2	66·1257	66·1257	8, 3	68·8628	68·8632	4, 7	71·1465	71·1482
42	72·7406	74·8180	76·9564	6, 6	69·7988	69·7991	2, 8	70·5715	70·5721	6, 6	72·8010	72·8024
44	75·9228	79·5013	80·7439	8, 3	72·4150	72·4151	3, 8	75·4388	75·4395	8, 4	78·6245	78·6262
46	81·3506	82·1832	84·5806	8, 4	76·1993	76·1998	6, 7	79·4468	79·4495	5, 7	79·6798	79·6818
48	83·1115	87·4113	87·6193	5, 8	79·7877	79·7894	2, 9	81·5921	81·5954	1, 9	84·4765	84·4795
50	86·5187	87·8702	90·6570	7, 6	82·7071	82·7075	8, 5	83·1369	83·1384	7, 6	85·4156	85·4172
52	88·7050	88·1290	92·3793	8, 5	83·1640	83·1644	9, 3	85·7599	85·7603	2, 9	87·2166	87·2198
54	90·1601	92·2529	93·8843	3, 9	85·3358	85·3367	7, 6	86·1421	86·1427	6, 7	90·2016	90·2041
56	93·2357	98·2948	99·8653	6, 8	90·3975	90·3995	7, 7	91·8056	91·8089	9, 4	95·2393	95·2414
58	101·5324	99·3509	103·6024	9, 4	93·0844	93·0850	9, 4	97·4506	97·4509	4, 9	98·3421	98·3459
60	103·6554	105·0269	107·4419	8, 6	97·6255	97·6260	5, 9	100·7894	100·7944	9, 5	101·4524	101·4539
62	104·1439	107·2459	109·5361	1, 10	101·0000	101·0000	6, 8	101·9613	101·9623	7, 7	102·7277	102·7309
64	107·4395	110·2558	112·3682	10, 2	102·1084	102·1084	1, 10	104·3350	104·3364	7, 8	108·6130	108·6202
66	109·2117	113·2181	113·4002	2, 10	104·0000	104·0000	8, 7	106·2286	106·2326	1, 10	110·2093	110·2129
68	112·5385	118·1677	118·6760	3, 10	109·0000	109·0000	6, 9	111·0757	111·0815	10, 4	113·9223	113·9248
70	116·9976	118·8332	123·0503	6, 9	111·8755	111·8767	7, 8	114·8125	114·8137	8, 7	117·2668	117·2707
72	119·6867	120·4467	124·2412	1, 11	112·6879	112·6921	9, 6	117·9478	117·9486	3, 10	117·7859	117·7900
74	121·1704	125·1186	127·5358	2, 11	115·5063	115·5107	10, 5	118·5523	118·5546	8, 8	122·7073	122·7154
76	123·1036	127·4946	129·4242	8, 8	117·7274	117·7300	2, 11	121·0010	121·0083	4, 10	124·4589	124·4634
78	125·9432	130·2648	133·9062	3, 11	120·2208	120·2256	7, 9	123·3699	123·3767	7, 9	129·7636	129·7691
80	128·8808	134·0916	135·1480	7, 9	124·7217	124·7232	3, 11	125·5788	125·5867	2, 11	130·0998	130·1111
82	131·0462	135·1955	140·6434	4, 11	126·8534	126·8588	5, 10	127·8460	127·8479	9, 7	133·8228	133·8278
84	132·6714	139·7435	142·0719	11, 3	129·3608	129·3610	4, 11	132·0340	132·0427	11, 4	134·6588	134·6618
86	140·2753	141·4383	145·1853	10, 6	133·4898	133·4905	11, 4	137·3746	137·3750	9, 8	138·9029	138·9122
88	141·3695	145·0920	146·1326	5, 11	135·4283	135·4344	6, 10	138·6832	138·6854	11, 5	141·0734	141·0755
90	144·4231	146·1340	149·1162	1, 12	136·4973	136·5004	5, 11	140·4019	140·4117	8, 9	144·2738	144·2801
92	149·0463	148·9634	150·8658	8, 9	139·5767	139·5785	9, 8	146·5538	146·5554	12, 2	146·2150	146·2152
94	152·0685	152·2232	154·1113	3, 12	144·2814	144·2849	12, 3	148·5577	148·5584	5, 11	148·9688	148·9841
96	153·4035	156·3219	160·0486	12, 2	146·0969	146·0970	6, 11	150·7168	150·7278	12, 3	152·8130	152·8138
98	154·5051	158·6586	161·1298	7, 10	149·0000	149·0000	2, 12	151·9421	151·9451	7, 10	156·2901	156·2965
100	157·1764	160·5299	164·6372	12, 3	152·3474	152·3476	3, 12	156·8423	156·8455	10, 8	157·2017	157·2120

105	166·0254	169·2790	170·2004	7, 11	158·4941	158·5020	7, 11	163·0081	163·0206	12, 5	163·9294	163·9317
110	169·2120	177·7151	181·3292	1, 13	168·7767	168·7777	2, 13	168·3880	168·4021	11, 7	172·9933	173·0009
115	179·5529	182·9883	186·6928	11, 8	174·0138	174·0174	13, 3	173·5119	173·5128	1, 13	179·3979	179·4085
120	186·0803	188·5097	193·2336	13, 4	180·7876	180·7888	6, 12	183·4089	183·4128	3, 13	187·0210	187·0324
125	193·1405	200·6407	204·0139	9, 11	189·5579	189·5682	5, 13	187·9665	187·9841	12, 7	195·6099	195·6190
130	201·7132	205·2093	209·8169	11, 9	196·2071	196·2097	14, 2	200·0759	200·0761	5, 13	202·3570	202·3700
135	209·8234	211·6020	215·2894	10, 10	200·0000	200·0000	13, 6	205·6947	205·6960	14, 4	209·0884	209·0928
140	214·9630	222·1650	224·1779	14, 4	207·7387	207·7400	8, 12	211·0847	211·0894	3, 14	216·6031	216·6261
145	220·5324	225·9773	228·9392	9, 12	215·0975	215·1033	4, 14	216·4171	216·4231	4, 14	223·1676	223·1924
150	226·9387	230·6764	233·8386	3, 15	220·3386	220·3496	5, 14	225·2811	225·2875	15, 2	227·1786	227·1789
155	236·5583	240·2365	243·7345	4, 15	227·1424	227·1539	11, 11	232·3154	232·3361	15, 3	233·6853	233·6866
160	242·2463	243·4727	248·6043	10, 12	233·9071	233·9135	6, 14	236·1307	236·1375	10, 12	240·4188	240·4388
165	249·8023	253·0464	258·4100	15, 5	243·7888	243·7899	5, 15	243·4891	243·5186	5, 15	248·1095	248·1466
170	259·0557	259·4536	263·5337	14, 8	248·5560	248·5609	12, 11	254·7255	254·7487	16, 2	258·1696	258·1700
175	267·0639	266·6128	272·2708	2, 16	255·4492	255·4545	15, 6	261·6103	261·6120	16, 3	264·6531	264·6545
180	270·4778	272·9381	280·2869	16, 3	264·3078	264·3082	7, 15	266·2503	266·2851	7, 15	270·6485	270·6903
185	277·5645	279·8796	285·7878	13, 10	269·0000	269·0000	16, 4	272·2617	272·2625	16, 5	275·5310	275·5348
190	283·2834	287·0638	291·0925	13, 11	275·9329	275·9499	8, 15	280·5690	280·6070	9, 14	284·8053	284·8480
195	292·1175	299·1544	302·5785	6, 16	287·1653	287·1718	15, 8	290·0473	290·0506	17, 2	291·1617	291·1621
200	299·0781	306·0460	308·4618	9, 15	290·8127	290·8285	17, 3	293·3850	293·3864	9, 15	301·0885	301·1359
205	302·2190	310·2393	315·4299	15, 9	299·8520	299·8562	14, 10	297·6553	297·6603	1, 17	307·2137	307·2434
210	310·9922	316·6969	322·2859	4, 17	302·4453	302·4524	14, 11	305·6640	305·6929	7, 16	311·1845	311·2180
215	318·3957	322·2642	326·2012	16, 8	308·3415	308·3472	13, 12	315·3785	315·3860	4, 17	321·6936	321·7263
220	331·0294	331·0622	331·7124	3, 18	314·9324	314·9634	17, 6	325·5434	325·5455	1, 18	327·4866	327·5651
225	333·5202	339·6844	342·9122	15, 10	325·0000	325·0000	17, 7	328·2878	328·3006	16, 9	333·6135	333·6291
230	338·5871	342·6898	347·5158	5, 18	330·4123	330·4459	15, 11	334·1902	334·2221	11, 15	339·5764	339·6302
235	346·2143	347·4022	352·7955	17, 7	335·1392	335·1448	18, 5	341·4239	341·4300	13, 13	343·0331	343·0605
240	355·3148	354·9175	361·0493	17, 8	341·2532	341·2595	14, 13	352·9766	353·0213	7, 17	353·6833	353·7228
245	361·5320	367·0702	370·4732	12, 15	353·0142	353·0337	12, 15	357·7669	357·8220	12, 15	361·8656	361·9230
250	366·1366	372·6974	375·4987	18, 6	357·1766	357·1787	18, 6	360·5150	360·5571	8, 17	368·2738	368·3165
255	371·5864	375·2814	382·3741	14, 13	363·1926	363·1968	19, 3	365·3424	365·3441	2, 19	370·2256	370·2826
260	379·0916	382·9253	388·7632	19, 3	369·2876	369·2881	19, 4	377·2212	377·2223	18, 8	378·1842	378·2028
265	386·5502	389·6243	394·4641	5, 19	376·2554	376·2724	11, 16	381·0500	381·0649	8, 18	386·0885	386·1963
270	397·0259	400·5129	405·9528	10, 17	385·8218	385·8350	17, 10	390·4184	390·4251	19, 6	395·2772	395·2853
275	402·5573	405·7496	410·6859	19, 6	394·1525	394·1549	19, 6	397·4893	397·4918	9, 18	402·1095	402·1435
280	408·2539	414·6846	419·3962	1, 20	401·0000	401·0000	12, 16	403·8940	403·9100	20, 3	408·5560	408·5581
285	414·0795	422·3519	427·5245	11, 17	406·6876	406·7024	9, 18	410·0978	410·1173	19, 8	414·9935	415·0133

TABLE 4

Continued

Mode number	SCCS	CCCS	CCCC	SSSS			SSCS			CSCS		
				m, *n*	Levy	DSC	*m*, *n*	Levy	DSC	*m*, *n*	Levy	DSC
290	422·8710	427·3200	432·3922	20, 4	411·5470	411·5495	20, 4	416·2104	416·2115	11, 17	423·9283	423·9836
295	431·2091	433·2551	439·0250	13, 16	419·4112	419·4231	18, 10	425·3523	425·3595	18, 10	428·0789	428·1037
300	434·5251	443·2319	445·5779	1, 21	424·1421	424·2012	5, 20	431·3839	431·4079	18, 11	436·7782	436·8472
305	441·7089	446·5759	452·9840	9, 19	431·7019	431·7229	20,6	436·4660	436·4688	21, 2	443·1379	443·1385
310	448·3505	455·5337	460·5279	6, 20	436·0000	436·0000	3, 21	442·6019	442·6992	1, 21	452·4999	452·6346
315	452·6848	460·3357	467·4353	14, 16	446·3054	446·3184	4, 21	449·2813	449·3816	14, 16	454·9206	454·9769
320	459·9795	467·0620	472·6467	10, 19	450·5456	450·5679	14, 16	455·5985	455·6169	17, 13	461·7019	461·7407
325	470·5609	473·1480	478·4578	18, 12	456·7939	456·8069	20, 8	464·8113	464·8164	4, 21	466·5860	466·7308
330	475·7456	482·0981	487·0854	16, 15	464·1308	464·1565	18, 12	469·8799	469·8912	21, 6	475·1293	475·2095
335	482·0119	487·1594	493·3773	11, 19	471·3871	471·4109	21, 6	477·4448	477·4477	6, 21	485·4344	485·5926
340	489·7528	494·9696	499·3016	15, 16	475·2027	475·2168	9, 20	486·8205	486·8487	2, 22	489·8872	490·0056
345	496·7324	501·7272	508·4043	8, 21	485·3466	485·4239	12, 19	493·0200	493·1325	22, 4	496·3351	496·3445
350	505·1933	505·7748	513·8137	5, 22	492·9870	492·9958	22, 4	500·1915	500·1929	19, 12	497·8361	497·8905
355	511·0710	512·5346	518·3251	17, 15	496·9444	496·9717	10, 20	505·6607	505·6903	12, 19	505·9416	506·0307
360	516·0737	519·5281	524·9950	22, 5	502·6504	502·6526	21, 9	509·6344	509·6679	16, 16	514·0845	514·1497
365	522·4722	528·7187	535·1678	15, 17	510.1135	510·1372	13, 19	517·3152	517·4361	18, 14	520·8361	520·9490
370	528·9912	539·0541	541·5440	10, 21	520·4902	520·5777	14, 18	524·3011	524·3272	22, 7	532·9152	532·9481
375	533·1641	545·0650	550·2103	22, 7	529·8193	529·8287	10, 21	530·0231	530·1591	23, 3	537·5050	537·5078
380	544·6004	548·9341	554·4183	20, 12	532·6093	532·6243	4, 23	536·6764	536·8195	21, 10	544·5828	544·6101
385	552·2454	553·9332	561·9001	23, 4	540·4887	540·4919	5, 23	545·3072	545·4548	23, 5	548·1684	548·1753
390	556·5796	561·5833	567·0817	12, 20	544·0000	544·0000	22, 8	548·7430	548·7490	14, 19	556·8998	557·0003
395	559·0348	568·7871	571·1712	9, 22	548·2930	548·3395	20, 13	554·0858	554·1607	23, 6	563·0055	563·0169
400	569·4677	580·0961	585·4931	6, 23	562·7405	562·7514	23, 6	565·4075	565·4110	20, 13	571·8974	571·9463
405	577·5210	587·1127	594·0277	2, 24	567·9882	568·0590	15, 19	571·9258	572·0655	6, 23	580·6557	580·7648
410	588·1051	591·2303	597·9346	17, 17	573·8185	573·8481	8, 23	582·8250	582·9925	24, 3	584·4909	584·4938
415	592·3373	597·3412	604·4563	24, 2	578·0685	578·0688	21, 12	586·6591	586·6731	17, 17	589·1197	589·2167
420	600·3249	604·6406	610·5207	24, 3	584·2640	584·2648	3, 24	592·9294	592·9758	1, 24	597·7266	597·8972
425	604·0895	609·2979	614·5590	22, 11	588·6134	588·6877	23, 9	597·2573	597·2962	23, 9	605·4688	605·5895
430	607·3204	620·8925	625·8772	6, 24	599·4217	599·5016	14, 20	601·0157	601·0521	13, 21	612·2763	612·5236
435	617·8615	625·0367	629·4318	20, 15	607·4580	607·4908	24, 6	612·3910	612·3948	22, 12	620·1006	620·1525
440	624·0660	629·7104	633·4925	12, 22	610·6755	610·7290	6, 24	619·6548	619·7041	12, 22	625·1883	625·3524

445	632·5485	639·7226	645·8082	22, 12	616·4506	616·4678	25, 2	629·0424	629·0429	6, 24	631·3951	631·5907
450	640·1736	642·7591	648·8495	15, 20	625·0000	625·0000	4, 25	632·0623	632·2606	18, 18	636·3183	636·5278
455	641·6193	646·0024	653·3339	24, 8	627·8499	627·8597	23, 11	635·4641	635·5266	4, 25	640·2079	640·4636
460	648·6133	653·9370	660·8269	25, 4	636·4577	636·4614	5, 25	640·7193	640·9230	5, 25	648·7815	649·0424
465	655·4382	663·6113	671·1634	9, 24	643·7006	643·7932	21, 15	649·6696	649·7841	20, 16	656·6297	656·7155
470	663·0659	670·6011	674·7578	24, 9	650·3957	650·4048	13, 22	658·8989	658·9461	11, 23	663·8043	663·9391
475	673·5774	676·4726	683·4940	19, 18	661·3006	661·3774	7, 25	663·8454	664·0636	19, 18	672·4919	672·7133
480	684·5933	687·5699	691·6864	22, 14	667·4606	667·5148	24, 10	677·0507	677·0620	25, 8	678·2019	678·2297
485	688·0551	690·2399	697·7084	18, 19	673·3370	673·3744	23, 13	682·0079	682·1007	24, 11	685·9693	686·0783
490	693·1304	697·5055	705·3575	26, 2	678·0664	678·0667	1, 26	685·6842	685·7468	2, 26	692·9498	693·1263
495	696·4076	705·0758	712·5757	20, 17	684·3830	684·4232	26, 4	692·1623	692·1642	21, 16	697·3099	697·4015
500	704·8269	707·9949	714·4310	15, 22	691·0521	691·1142	3, 26	693·6034	693·6670	17, 20	702·1971	702·3109
505	709·9460	714·0519	721·0430	23, 13	695·7961	695·8070	19, 19	705·3314	705·5151	20, 18	710·7078	710·9412
510	719·4768	722·6896	732·6513	12, 24	705·8127	705·9232	10, 25	713·1626	713·4111	19, 19	719·5365	719·6716
515	725·0901	736·9088	741·0569	23, 14	712·2662	712·3244	1, 27	720·9904	721·2484	25, 10	728·0713	728·1074
520	734·1347	741·0433	748·4116	14, 23	722·3793	722·3974	23, 14	727·0368	727·0600	16, 22	734·7848	734·9824
525	736·6802	746·1487	755·2624	26, 8	727·7772	727·7881	25, 11	730·9976	731·0690	14, 23	737·5145	737·6712
530	744·8118	752·6849	760·4737	8, 26	732·2901	732·3325	4, 27	735·4409	735·7093	23, 15	741·4814	741·5892
535	749·9083	760·4058	766·8184	27, 4	740·4314	740·4355	20, 19	743·7332	743·8369	26, 9	752·1437	752·1775
540	754·5729	765·3767	772·3111	12, 25	744·4146	744·5257	27, 5	745·9413	745·9537	25, 12	760·5087	760·5714
545	759·4098	771·7879	776·9395	26, 9	750·3308	750·3413	22, 17	755·3391	755·5063	15, 23	766·0794	766·2445
550	774·0573	779·7905	789·4278	25, 12	757·2516	757·4074	27, 7	767·0913	767·1194	19, 20	773·4699	773·5980
555	781·8248	790·3085	792·8347	27, 6	762·0172	762·0217	24, 14	773·9669	773·9914	27, 8	782·0239	782·0741
560	785·5531	792·3053	803·2611	4, 28	771·8877	772·0743	13, 25	780·1945	780·4834	10, 26	786·6071	786·8227
565	793·6507	798·3304	805·9863	23, 16	778·5112	778·5374	21, 19	784·1569	784·3657	2, 28	791·7823	792·2414
570	799·9020	804·7083	810·8635	24, 15	782·9502	782·9911	27, 8	793·6126	793·6210	3, 28	796·5224	796·8205
575	806·7297	807·2894	814·5252	11, 26	789·0100	789·0581	23, 17	799·8634	800·0415	28, 5	803·0218	803·0313
580	810·0197	817·1604	822·3241	28, 3	792·2507	792·2518	20, 20	804·1550	804·2050	26, 12	811·3370	811·4033
585	818·5824	823·1716	831·0779	27, 9	803·3015	803·3127	22, 18	811·2765	811·3180	28, 6	817·7699	817·7860
590	829·9237	834·1361	838·9651	12, 26	811·9072	811·9576	26, 12	821·3802	821·3995	17, 23	829·2182	829·4015
595	834·1195	843·3047	849·9852	28, 6	817·0052	817·0100	12, 26	827·5098	827·5901	7, 28	834·5436	835·0528
600	839·3574	846·7131	853·4540	19, 22	826·2780	826·3537	1, 29	832·3263	832·6702	23, 18	837·6064	837·8753
605	842·5831	850·5206	857·7223	2, 29	830·5282	830·6128	18, 23	836·0845	836·3792	29, 2	843·1105	843·1116
610	847·4195	857·1863	863·2819	9, 28	835·5654	835·7279	21, 20	845·0298	845·0371	1, 29	850·2026	850·5050
615	856·2771	864·0267	869·8593	26, 13	842·6921	842·7060	28, 8	848·5917	848·6006	13, 26	854·2553	854·4981
620	862·1058	873·3889	878·8601	18, 23	850·1627	850·1870	23, 18	856·1740	856·2178	27, 12	864·1761	864·2463
625	871·0358	876·9244	886·9114	21, 21	856·4913	856·6718	21, 21	863·5852	863·8574	24, 17	873·0958	873·2782

TABLE 4

Continued

Mode number	SCCS	CCCS	CCCC	SSSS			SSCS			CSCS		
				m, *n*	Levy	DSC	*m*, *n*	Levy	DSC	*m*, *n*	Levy	DSC
630	878·5036	883·9352	889·8196	27, 12	861·1398	861·1633	19, 23	872·4064	872·7184	20, 22	876·5939	876·8398
635	886·6020	890·6181	901·0765	29, 6	873·9939	873·9990	7, 29	878·7412	878·9789	24, 18	883·9863	884·2668
640	893·7671	899·8684	907·6886	23, 19	877·7752	877·7756	25, 16	883·4218	883·4578	29, 7	888·9015	888·9562
645	895·8049	905·8644	913·8143	29, 7	886·5236	886·5396	28, 11	889·4045	889·4902	12, 27	897·3872	897·6372
650	911·0146	912·8305	921·7823	15, 26	892·5830	892·6416	24, 18	903·0765	903·1226	17, 25	904·3233	904·7126
655	913·5282	924·3004	930·4580	22, 21	899·0870	899·2787	22, 21	905·9859	906·2744	30, 4	911·9937	912·0094
660	919·1890	928·6426	934·3608	9, 29	906·9307	907·0279	20, 23	910·7413	911·0714	28, 12	919·0252	919·0994
665	926·2440	931·9714	943·8264	27, 14	911·5884	911·6636	30, 5	916·8452	916·8600	9, 29	928·1113	928·4560
670	935·3045	941·9627	949·0258	14, 27	920·1907	920·2623	10, 29	928·2189	928·6416	24, 19	932·6050	932·7825
675	941·2356	945·4086	952·7578	25, 18	923·8487	923·9502	26, 16	934·3466	934·3845	16, 26	939·8286	940·1047
680	946·3794	952·2070	957·1053	20, 23	926·0538	926·0818	30, 6	936·3145	936·3348	10, 29	946·6711	947·0257
685	951·1553	962·5665	971·2059	6, 30	936·0000	936·0000	19, 24	942·6753	942·7571	13, 28	949·5037	950·1413
690	956·5453	967·5197	977·4251	29, 11	944·6019	944·6634	23, 21	950·4064	950·7116	23, 21	962·6380	962·9772
695	959·9986	978·1630	981·4464	7, 30	949·0000	949·0000	7, 30	958·6175	958·7363	26, 17	972·3046	972·5192
700	973·6080	981·0835	986·3030	17, 26	956·3610	956·4259	31, 3	965·2055	965·2094	28, 14	975·4771	975·7481
705	976·1823	988·1214	994·3856	31, 2	963·0622	963·0626	16, 27	968·7326	969·1640	1, 31	977·5199	978·1486
710	981·9008	991·4305	1001·0105	12, 29	969·5159	969·6231	5, 31	974·8993	975·3711	26, 18	982·8571	983·1604
715	991·6951	995·2740	1004·8952	30, 9	974·2242	974·2375	28, 14	981·7257	981·7564	12, 29	989·7209	990·0979
720	998·7441	1007·5371	1011·1605	31, 5	979·5657	979·5696	28, 15	990·0841	990·2603	5, 31	1000·5178	1001·1803
725	1005·7673	1012·2639	1019·9723	28, 15	990·5621	990·6117	24, 21	996·8467	997·1691	9, 30	1006·9141	1007·2098
730	1011·4853	1019·5486	1026·8804	8, 31	997·2863	997·6126	30, 10	1000·8549	1000·8709	6, 31	1011·0708	1011·2935
735	1014·2062	1027·3531	1036·5169	1, 32	1002·1786	1002·3486	18, 26	1006·5431	1006·7415	22, 23	1002·1966	1022·4333
740	1025·5220	1032·7942	1039·4549	16, 28	1007·8735	1008·1469	23, 22	1017·4428	1017·5183	32, 2	1026·1038	1026·2538
745	1035·8438	1042·3177	1046·8287	17, 27	1012·8026	1012·8912	31, 9	1028·1959	1028·2030	32, 3	1032·4092	1032·4141
750	1043·3393	1045·1721	1052·8211	29, 14	1023·3011	1023·3854	18, 27	1035·3280	1035·8036	3, 32	1035·7274	1035·9534
755	1048·8044	1048·8059	1058·4199	27, 18	1027·4730	1027·5830	32, 4	1040·1320	1040·1347	17, 27	1040·1735	1040·4971
760	1053·5644	1052·1426	1064·8561	28, 16	1033·1884	1033·2245	30, 12	1045·2134	1045·2373	11, 30	1046·2697	1046·5841
765	1056·2153	1062·9824	1073·3860	21, 25	1038·9890	1039·1797	10, 31	1047·7204	1048·2597	9, 31	1054·3174	1055·0584
770	1064·9284	1072·8166	1076·2336	12, 30	1044·0000	1044·0000	12, 30	1052·9478	1053·0817	17, 28	1065·4822	1066·2400
775	1072·4583	1075·8039	1084·4626	11, 31	1053·2360	1053·5969	31, 10	1061·8289	1061·8458	15, 29	1069·1842	1069·6014

780	1077·6812	1087·4417	1097·0456	8, 32	1064·5475	1064·7328	27, 19	1069·1512	1069·4454	18, 27	1074·7082	1075·1159
785	1082·5435	1095·3307	1103·4164	32, 7	1069·4311	1069·4504	26, 20	1079·4806	1079·5762	26, 20	1086·2853	1086·4730
790	1088·1393	1103·2663	1108·5390	27, 19	1077·3229	1077·3853	7, 32	1083·3068	1083·4592	11, 31	1092·8526	1093·6496
795	1096·4501	1107·8388	1117·2280	28, 18	1082·3019	1082·4162	12, 31	1090·5670	1091·1454	33, 3	1097·4018	1097·4070
800	1106·7860	1114·1883	1121·9412	26, 21	1089·6003	1089·8401	26, 21	1095·7864	1096·1447	33, 4	1100·9098	1100·9281
805	1111·7405	1117·5735	1127·5391	3, 33	1094·8861	1094·9271	14, 30	1104·6358	1104·7778	19, 27	1111·2398	1111·6012
810	1117·8467	1123·2690	1130·8998	33, 4	1100·3718	1100·4175	29, 17	1109·4472	1109·6968	2, 33	1116·7049	1117·1167
815	1121·7387	1129·1098	1138·4121	33, 5	1107·5533	1107·5576	17, 29	1112·6597	1113·2273	10, 32	1124·2025	1124·7963
820	1126·4836	1141·8329	1148·6350	11, 32	1121·0455	1121·2442	18, 28	1115·2645	1115·5479	17, 29	1132·1279	1132·5760
825	1136·7659	1148·1725	1157·3127	29, 17	1124·2193	1124·3032	7, 33	1125·5888	1126·2168	27, 20	1139·0190	1139·2161
830	1142·0521	1152·2718	1162·4567	31, 13	1127·5445	1127·5643	23, 25	1133·3417	1133·6218	11, 32	1144·6846	1145·2924
835	1152·0508	1159·8463	1171·3492	7, 33	1134·8055	1134·8499	18, 29	1146·9589	1147·5525	26, 22	1149·8586	1150·1690
840	1159·1448	1168·8783	1176·0867	27, 21	1142·2610	1142·5136	11, 32	1154·8071	1154·9725	32, 12	1158·5058	1158·9882
845	1171·2453	1172·1837	1180·6320	18, 29	1148·5814	1148·7161	31, 14	1158·5780	1158·6135	33, 9	1164·5983	1164·6481
850	1173·3622	1180·7424	1188·9095	22, 26	1150·8154	1150·8993	22, 26	1165·9381	1166·0560	34, 4	1167·8853	1167·9045
855	1177·4331	1186·9991	1196·8067	34, 2	1158·0603	1158·0608	32, 12	1169·1436	1169·1700	16, 30	1179·4083	1179·7836
860	1183·6391	1194·8926	1202·0172	9, 33	1166·7442	1166·7912	32, 13	1174·7412	1174·8967	21, 27	1190·2992	1190·7034
865	1189·8499	1205·0809	1211·0214	34, 5	1174·5477	1174·5521	29, 19	1180·3086	1180·6342	28, 20	1193·7632	1193·9700
870	1196·6074	1208·4755	1220·3771	19, 29	1185·4234	1185·5635	33, 10	1189·7812	1189·7999	33, 11	1196·3965	1196·5772
875	1203·7607	1213·0250	1223·7029	17, 30	1189·0000	1189·0000	33, 11	1193·6296	1193·7012	30, 18	1204·9893	1205·3362
880	1209·5983	1220·2888	1226·3927	33, 11	1192·1927	1192·2685	13, 32	1202·5118	1202·6857	10, 33	1210·9595	1211·4288
885	1216·8410	1225·2416	1231·3423	28, 21	1196·9341	1197·1999	1, 35	1214·3323	1215·0666	32, 14	1213·9894	1214·3148
890	1227·2725	1228·9394	1236·3500	8, 34	1202·2565	1202·5760	31, 16	1219·0256	1219·0740	16, 31	1223·4626	1224·4454
895	1232·7542	1239·1239	1243·7499	34, 8	1207·5785	1207·5943	34, 9	1222·9193	1222·9931	11, 33	1231·6149	1232·0964
900	1237·2340	1247·4331	1252·9083	9, 34	1219·0537	1219·3825	32, 15	1228·9886	1229·1861	32, 15	1234·2752	1234·6378
905	1242·6543	1250·4160	1261·6648	20, 29	1224·2666	1224·4832	21, 28	1231·7931	1231·9357	35, 5	1243·8879	1243·9018
910	1246·8026	1260·3384	1267·0726	32, 15	1230·2596	1230·3186	23, 27	1236·8943	1237·4984	29, 20	1250·5176	1250·7344
915	1251·8596	1264·3895	1274·2340	10, 34	1237·8321	1238·1713	35, 5	1241·7220	1241·7411	17, 31	1255·5012	1256·5287
920	1261·3704	1269·2183	1280·2466	31, 17	1243·9969	1244·0925	26, 24	1256·7347	1256·7789	35, 6	1258·5499	1258·5733
925	1268·4277	1276·0939	1286·0994	29, 21	1253·6194	1253·8986	34, 11	1260·4994	1260·6163	27, 23	1265·4381	1265·7381
930	1273·8098	1282·1229	1292·8277	34, 10	1256·0000	1256·0000	18, 31	1266·5866	1266·8507	16, 32	1276·8019	1277·4953
935	1281·2836	1288·6475	1296·2808	34, 11	1259·1039	1259·1835	22, 28	1274·6415	1274·7894	13, 33	1278·8696	1279·3790
940	1292·5939	1294·9386	1307·1277	26, 25	1272·8802	1273·0224	33, 14	1286·4920	1286·5310	8, 35	1286·8019	1287·8249
945	1301·1504	1307·4166	1314·5164	12, 34	1281·3390	1281·5998	28, 23	1290·0180	1290·5156	23, 28	1299·4556	1300·4292
950	1309·1072	1315·6961	1322·9178	17, 32	1287·8453	1288·0814	15, 33	1297·2303	1298·0332	25, 26	1304·7720	1305·1801
955	1312·4518	1321·7535	1330·1736	3, 36	1294·7860	1294·9211	19, 31	1302·8868	1303·2024	30, 20	1309·2819	1309·9083
960	1315·4928	1326·0960	1335·0498	20, 30	1300·0000	1300·0000	20, 30	1307·6670	1307·8388	2, 36	1317·9806	1318·4696

TABLE 4

Continued

Mode number	SCCS	CCCS	CCCC	SSSS			SSCS			CSCS		
				m, *n*	Levy	DSC	*m*, *n*	Levy	DSC	*m*, *n*	Levy	DSC
965	1319·5397	1330·9557	1339·8576	13, 34	1306·0704	1306·4470	2, 36	1311·9981	1312·1207	3, 36	1322·8791	1323·5265
970	1330·3220	1333·0653	1344·4725	28, 23	1309·6402	1309·6877	23, 28	1319·4933	1319·6465	12, 34	1325·5959	1326·6567
975	1333·5715	1342·5238	1352·7195	36, 5	1314·5373	1314·5423	29, 22	1328·7881	1328·8856	4, 36	1329·7383	1330·3909
980	1342·7558	1348·4855	1357·9087	24, 28	1324·7925	1325·0000	36, 6	1332·2628	1332·2703	11, 35	1342·0414	1342·7022
985	1351·6363	1357·5295	1366·2000	36, 6	1328·9314	1328·9389	6, 36	1343·7686	1344·0069	24, 28	1345·5034	1346·5156
990	1358·2280	1366·4389	1374·3525	33, 16	1337·9301	1337·9774	32, 18	1350·4499	1350·5167	35, 12	1359·1872	1359·2910
995	1364·3538	1374·4672	1382·2903	26, 26	1342·4080	1342·5100	18, 32	1356·7140	1356·9204	12, 35	1364·3775	1365·2095
1000	1369·2552	1381·0624	1389·9940	35, 12	1356·8079	1356·8426	34, 15	1360·5185	1360·7578	37, 2	1371·0951	1371·0968
1050	1437·6122	1447·4895	1458·5268	3, 38	1415·0982	1415·7326	32, 20	1426·9667	1427·2188	30, 23	1435·5155	1436·0583
1100	1500·6425	1509·7491	1517·4442	22, 32	1481·8064	1482·0826	6, 38	1492·4481	1492·7434	22, 32	1501·1753	1502·0017
1150	1567·5806	1575·3418	1586·1324	32, 23	1549·4536	1549·5135	39, 6	1557·2428	1557·2514	11, 38	1566·0395	1567·7772
1200	1637·0091	1643·1093	1656·1389	22, 34	1618·2533	1618·5258	39, 11	1624·9419	1625·0867	40, 6	1633·4389	1633·6600
1250	1700·1000	1711·1009	1721·9671	6, 41	1681·4439	1682·3791	25, 33	1690·3239	1690·7055	41, 5	1699·8102	1700·3936
1300	1767·6902	1776·7603	1783·9556	12, 40	1744·0000	1744·0002	34, 25	1754·2736	1755·0636	42, 2	1766·0885	1766·4131
1350	1830·1752	1842·3494	1851·2220	33, 27	1810·4950	1810·7462	18, 39	1825·0047	1825·9448	8, 42	1830·4833	1832·1385
1400	1890·8284	1909·3085	1917·4154	5, 43	1869·9265	1870·0478	41, 14	1878·2220	1878·4306	4, 43	1895·7093	1895·9038
1450	1962·7904	1976·7864	1989·8175	21, 39	1940·4099	1940·8075	17, 41	1950·2154	1952·0381	21, 39	1965·8409	1967·2113
1500	2027·9135	2039·2387	2051·5082	19, 41	2002·0587	2003·3177	3, 45	2018·8270	2020·8887	20, 40	2031·6549	2032·7698
1550	2097·2377	2105·6223	2113·4665	15, 43	2069·6350	2069·7832	36, 28	2084·9048	2085·2504	11, 44	2092·3877	2094·5260
1600	2156·2752	2169·2275	2176·9239	43, 17	2130·9179	2131·0951	14, 44	2145·6295	2146·2143	45, 12	2158·4143	2158·5668
1650	2221·9374	2241·5196	2255·2038	45, 14	2205·7918	2205·9592	47, 2	2213·0225	2213·0299	46, 11	2221·3417	2221·6442
1700	2289·4482	2306·8086	2315·8906	39, 28	2265·6862	2266·2476	12, 46	2274·5854	2275·2657	18, 44	2291·5511	2293·4724
1750	2358·1398	2366·5579	2377·7901	15, 46	2327·2727	2327·7033	5, 48	2344·8899	2345·6589	48, 8	2356·1003	2356·7416
1800	2422·4828	2433·3676	2448·4696	30, 39	2398·0010	2398·5065	47, 14	2406·0743	2406·1450	32,37	2419·2081	2420·7230
1850	2486·8311	2498·0095	2508·7972	27, 42	2458·9708	2459·7448	41, 28	2469·4484	2469·7186	27, 42	2485·1685	2487·4745
1900	2551·0738	2559·3623	2573·8605	32, 39	2521·7025	2522·2352	50, 6	2536·1897	2536·2268	26, 43	2548·3472	2550·1356
1950	2622·5825	2632·3049	2644·4858	33, 39	2586·5563	2587·1031	28, 43	2605·3505	2606·9823	19, 47	2613·0061	2615·1185
2000	2683·6837	2699·8622	2713·8441	36, 37	2656·0497	2656·5966	17, 49	2668·3420	2669·2634	50, 14	2685·8444	2686·7491
2050	2746·1783	2759·2553	2770·5324	35, 39	2722·2708	2722·5531	49, 19	2734·8185	2735·5192	38, 36	2743·8754	2745·5457
2100	2811·6338	2832·4824	2839·8570	11, 52	2787·0938	2788·4922	47, 25	2802·3497	2803·3111	20, 49	2809·0965	2811·1754

2150	2874·6009	2892·8008	2909·2400	53, 7	2854·0575	2854·1951	22, 49	2860·2823	2863·6560	25, 47	2874·4761	2877·9934
2200	2946·2301	2965·9832	2979·2936	16, 52	2921·3320	2922·8028	38, 39	2931·4817	2932·2274	10,53	2945·9180	2948·6489
2250	3010·6255	3030·7195	3041·4927	22, 50	2984·0000	2984·0217	50, 23	2998·0381	2999·1537	53, 15	3016·8615	3017·3392
2300	3070·8069	3087·3906	3102·3116	29, 47	3041·0315	3041·7727	7, 55	3054·8104	3059·9772	38, 40	3068·7425	3070·5196
2350	3145·5599	3157·1573	3173·1494	12, 55	3118·2045	3120·7374	11, 55	3125·5577	3128·2633	56, 2	3138·0764	3138·5971
2400	3205·7635	3219·0756	3229·1342	25, 51	3175·6761	3176·0207	26, 50	3189·9434	3190·5887	19, 53	3204·1430	3205·6910
2450	3268·6674	3289·4802	3304·7753	50, 28	3242·8708	3243·5897	57, 3	3253·1100	3254·1262	39, 42	3270·4922	3273·2042
2500	3333·9007	3353·1464	3368·6337	55, 17	3306·1731	3306·6436	37, 44	3315·0637	3317·1609	54, 21	3333·3655	3335·6691
2550	3407·9505	3414·4254	3431·2228	8, 58	3369·5558	3372·1666	3, 58	3392·3196	3393·5965	5, 58	3396·6313	3402·2793
2600	3469·2063	3482·6502	3498·2292	56, 18	3431·9175	3432·4575	49, 33	3452·9156	3455·3828	58, 10	3465·3744	3466·2013
2650	3530·5097	3543·5217	3559·8159	57, 16	3497·2031	3498·5541	7, 59	3509·5356	3511·8354	15, 57	3528·9020	3532·8591
2700	3604·1577	3619·2268	3637·5236	37, 47	3567·9110	3568·8937	57, 19	3581·5379	3584·8996	43, 42	3596·5596	3600·9286
2750	3661·3988	3680·2312	3699·2364	53, 29	3629·6898	3631·9071	60, 7	3636·9359	3639·6611	2, 60	3658·5339	3665·0686
2800	3729·4406	3745·5705	3760·8857	24, 56	3694·7399	3697·2550	53, 30	3713·0963	3715·1311	19, 58	3724·8758	3731·4343
2850	3790·7703	3809·5789	3831·3499	59, 17	3761·9770	3763·2550	29, 54	3771·9071	3773·9385	6, 61	3786·7857	3791·4956
2900	3858·9079	3878·1616	3890·8410	43, 45	3824·0267	3825·7432	57, 25	3839·7124	3842·3773	54, 31	3852·4187	3858·5830
2950	3919·6198	3935·7822	3954·2839	58, 23	3888·5717	3889·7137	17, 60	3907·8493	3911·2848	49, 39	3913·1083	3921·7189
3000	3986·6197	4008·7738	4023·3487	51, 37	3958·9264	3959·9153	59, 22	3967·0804	3970·7934	25, 58	3983·6175	3986·6769
3050	4060·8599	4070·8838	4087·7725	63, 8	4020·3033	4021·0175	63, 8	4033·2674	4038·7417	48, 42	4049·3605	4054·6124
3100	4126·9869	4145·2442	4163·1370	17, 62	4087·2157	4090·9114	62, 16	4101·0699	4105·9734	25, 59	4115·2901	4122·1958
3150	4190·4832	4204·1267	4222·2439	9, 64	4144·5074	4147·3556	28, 58	4164·5176	4170·0034	23, 60	4178·9669	4188·2469
3200	4250·1308	4270·1606	4284·7680	12, 64	4207·0874	4214·5730	65, 2	4229·0163	4237·1643	65, 5	4243·6444	4252·4203
3250	4316·1052	4334·8454	4348·6594	54, 37	4273·5339	4277·3294	60, 27	4292·3226	4298·5085	34, 56	4309·0050	4313·8749
3300	4390·7158	4402·3295	4415·6126	60, 28	4341·7527	4346·6629	26, 61	4367·1211	4373·6676	63, 20	4373·9198	4384·9027
3350	4448·3214	4464·3054	4483·4363	21, 63	4403·6429	4409·0679	65, 14	4421·7861	4431·1610	7, 66	4437·5186	4447·0163
3400	4519·0359	4541·6139	4556·5269	12, 66	4480·9879	4487·9176	17, 65	4488·1510	4503·9916	64, 21	4510·8424	4519·7838
3450	4579·1942	4601·6366	4616·0424	53, 42	4534·5563	4543·5745	63, 24	4547·3141	4558·2618	4, 67	4572·0996	4583·2302
3500	4656·7570	4673·6958	4691·6018	11, 67	4600·1944	4607·6831	65, 20	4626·5808	4630·0394	2, 68	4637·6016	4650·3611
3550	4711·4587	4728·2170	4746·8175	46, 51	4657·0048	4669·5400	66, 18	4681·2687	4691·9485	67, 15	4696·0713	4710·8888
3600	4784·4396	4802·7918	4824·6480	56, 40	4736·0000	4746·6365	40, 56	4749·8663	4765·9312	55, 42	4767·6590	4777·7718
3650	4841·8150	4866·7943	4882·7444	8, 69	4790·3349	4804·0634	50, 48	4813·6885	4823·8699	52, 46	4823·6735	4839·5427
3700	4914·2002	4932·6769	4948·0759	55, 43	4867·5908	4873·1238	46, 53	4883·0760	4895·9283	67, 20	4893·6441	4908·3609
3750	4981·9171	5006·9416	5026·7483	14, 69	4921·8860	4945·2827	56, 43	4940·2537	4965·7515	45, 54	4962·2796	4981·1613
3800	5043·0665	5066·4550	5080·2091	60, 38	4989·2290	5003·4140	65, 28	5012·0172	5023·3740	66, 26	5026·2237	5042·9072
3850	5110·2056	5138·8761	5160·4785	71, 4	5052·2304	5075·7289	7, 71	5065·6727	5089·1986	66, 27	5088·6875	5113·0970
3900	5177·9226	5200·8164	5215·8743	34, 63	5118·0454	5132·1801	47, 54	5137·1178	5153·4488	9, 71	5156·0675	5182·2055
3950	5245·3622	5269·9287	5285·4414	70, 17	5180·5336	5203·8291	42, 59	5204·5800	5230·8359	67, 27	5221·4378	5249·9074

TABLE 4

Continued

Mode number	SCCS	CCCS	CCCC	SSSS			SSCS			CSCS		
				m, *n*	Levy	DSC	*m*, *n*	Levy	DSC	*m*, *n*	Levy	DSC
4000	5314·4428	5333·6821	5353·9859	52, 51	5242·4697	5265·6281	34, 64	5269·7221	5290·4119	72, 10	5285·1096	5312·9519
4050	5388·1658	5400·0014	5424·8405	61, 40	5321·0000	5336·8693	11, 72	5328·5891	5363·9353	63, 37	5351·3315	5381·6271
4100	5450·2563	5472·9220	5494·9900	50, 54	5376·5010	5410·2826	73, 8	5393·2309	5424·6661	46, 57	5406·7693	5451·3247
4150	5515·1820	5539·4619	5556·8891	61, 42	5445·6112	5474·0725	40, 62	5460·0263	5494·5235	72, 18	5482·0950	5514·6546
4200	5590·1693	5619·8371	5636·0140	71, 22	5502·2556	5544·7612	68, 30	5527·3020	5566·0082	47, 58	5545·7040	5592·7633
4250	5653·3193	5681·3871	5701·2423	60, 45	5571·9065	5605·2899	17, 73	5589·9005	5631·9856	15, 73	5604·5024	5660·1477
4300	5723·3646	5749·5667	5775·4628	75, 3	5633·1974	5679·3678	27, 70	5649·9875	5706·6672	17, 73	5667·9758	5730·3838
4350	5795·9728	5809·3383	5842·5671	12, 75	5700·3717	5744·9874	58, 49	5716·9906	5765·2719	49, 58	5735·7963	5791·3588
4400	5861·6163	5878·6781	5903·7035	3, 76	5763·4811	5814·9659	67, 36	5789·7026	5833·9198	53, 55	5802·2703	5858·5313
4450	5934·6105	5964·0685	5986·1494	65, 40	5825·0000	5893·1612	54, 54	5843·1780	5915·3072	18, 74	5859·5957	5934·6093
4500	6000·3392	6022·2732	6050·4123	58, 51	5900·1167	5948·9682	73, 25	5916·7632	5975·6228	51, 58	5933·9283	5997·3326
4550	6070·5788	6100·7402	6120·9160	76, 14	5955·5740	6019·0781	13, 76	5969·7846	6052·6835	73, 26	5998·4468	6078·1663
4600	6145·9118	6174·1293	6197·7397	58, 52	6021·4253	6101·0837	64, 44	6039·0173	6117·7805	23, 74	6062·1854	6146·3605
4650	6207·7303	6239·7222	6263·2812	75, 22	6086·1485	6159·1151	75,22	6110·6614	6178·4925	60, 50	6126·8798	6222·0033
4700	6290·9730	6315·4143	6341·6734	75, 23	6149·2133	6230·0401	55, 56	6172·7194	6259·1488	76, 21	6188·6090	6293·6712
4750	6357·4863	6379·4446	6414·1568	33, 72	6217·3489	6298·0820	4, 79	6230·4911	6329·4775	78, 13	6251·2812	6358·8760
4800	6428·7018	6448·6788	6478·1345	29, 74	6275·5481	6370·5530	43, 67	6295·3818	6405·9228	79, 9	6315·3684	6429·5582
4850	6497·0564	6532·1630	6558·6993	12, 79	6345·1201	6451·1858	76, 25	6363·3312	6482·8341	24, 76	6384·9855	6498·3638
4900	6569·5066	6593·1167	6622·0860	80, 4	6411·2168	6512·0510	2, 80	6430·6810	6539·8391	75, 29	6451·3270	6568·6800
4950	6641·1211	6669·1045	6696·5692	77, 24	6478·8055	6594·9098	17, 79	6500·1648	6612·6823	16, 79	6516·7796	6645·8825
5000	6727·4765	6750·0937	6779·9501	75, 31	6537·1404	6674·7620	58, 57	6562·5454	6692·5416	80, 14	6582·8559	6722·0474

Figure 4 that all cases have a very similar trend of convergence. Such a similarity confirms again that the DSC algorithm is insensitive to boundary and support conditions.

3.2.2. *Comparison studies*

A common feature in Cases 1–3 is that they have two parallel edges that are simply supported. These cases can be treated by using the Levy method. The latter has been used to compute the exact eigenvalues of the first 10 000 modes for each of the three cases. These eigenvalues are used to provide a detailed assessment of the DSC algorithm for two-span plates. For a comparison, both the DSC solutions and the Levy ones are plotted in Figures 5, 6 and 7 for Cases 1, 2 and 3 respectively. The relative errors of the DSC algorithm are also included in these figures. These figures confirm the consistence of the DSC algorithm for all the three solvable cases as both the magnitude and trend of the error are essentially identical to each other. In general, the relative errors are extremely small for the first 3000 modes. The first 4000 modes are still reliable for most engineering purpose. In all cases, the errors increase to near 2% when the mode number reaches 5000. Since the first 4500 DSC modes computed by using the grid of 101^2 points have $<1\%$ relative errors, it is recommended that the DSC prediction associated with appropriate plate theories can be used to analyze high-frequency vibration of two-span plates and the results can be used in most engineering designs.

Obviously, the present results are the best ever obtained for these cases. It is noted that in case a better precision is required, it is very robust to fulfill such a requirement by increasing the number of the DSC grid points.

3.2.3. *Case studies*

The convergence studies and error analyses have confirmed the validity and accuracy of the DSC algorithm for the high-frequency analysis of two-span plates. In particular, we have shown that DSC algorithm is insensitive to boundary and support conditions. Therefore, the DSC results are valuable for more general plate analysis where the analytical or exact solution is unavailable. In the rest of this subsection, we report more detailed frequency parameters which are unavailable in any existing literature, due to the lack of stable and reliable numerical methods.

As the Levy solutions for high-frequency vibration of Cases 1–3 have not been reported previously, they are very valuable for objectively calibrating new numerical methods which are potentially useful for high-frequency analysis. To this end, we have listed in Table 4 a selected set of these Levy solutions. The detailed node information for the Levy solution is also given in Table 4.

The DSC results for Cases 4–6 are of benchmark quality for their first 5000 modes. Obviously, these DSC results are valuable for the numerical test of other potential methods. Therefore, selected DSC frequency parameters are reported in Table 4 for all the six cases up to mode 5000.

4. CONCLUSION

This paper introduces a novel computational algorithm for the analysis and prediction of high-frequency vibrations. The lack of reliable numerical methods for such analysis and prediction has been a long standing problem due to numerical round-off in conventional numerical methods. In practical engineering analysis and design, there are pressing demands for reliable theoretical prediction of high-frequency vibrations [1]. We

demonstrate that the discrete singular convolution (DSC) algorithm [14–16] is an extremely promising approach for solving these classes of problems. The theoretical foundation of the DSC algorithm is the mathematical theory of distribution and wavelet analysis. The computational philosophy of the DSC algorithm is briefly discussed in the context of the present application. Both beams and two-span plates are treated in this work. The Levy method is employed to provide a cross validation of the present prediction.

To test the numerical stability of the DSC algorithm, a beam which is free of axial forces is employed in this study. The availability of an analytical solution for this problem provides an ideal benchmark for the proposed DSC approach. Convergence studies are carried out with a number of grid points ranging from 1001 to 10 001. At the final grid ($N = 10\,001$), extremely accurate results, which are up to 12 significant figures, are obtained for the first 2000 modes. This level of accuracy has not been previously reported to our knowledge. All the relative errors for the first 7161 modes are $<1\%$. Such an accuracy is believed to be reliable for the purpose of most engineering designs as the modal shapes are also found to be correct at this level of accuracy. Remarkably, the DSC algorithm has not encountered any numerical instability in all of our computations. Therefore, in case a higher level precision is desirable for a practical application, one can easily enlarge the number of grid points to achieve a better prediction.

Rectangular plates with internal supports are considered to further validate the proposed DSC algorithm for the prediction of high-frequency vibrations. The internal supports are implemented to demonstrate the possibility of frequency parameter optimization and control. Six cases of plates which consist of simply supported edges and clamped edges, and their combinations, are studied in the present work. Convergence studies are carried out for all the six plates, while, more details are given to an SSCS plate and a CCSC plate. Numerical results are carefully validated by the Levy solutions for two-span SSSS, SSCS, and CSCS plates. It is found that the DSC results are remarkably accurate for these three plates. With the grid of 101^2 points, the relative errors for the first 2000 modes are all smaller than 0·04% for all the three cases. Moreover, the first 4500 modes and the first 5000 modes (i.e., half of the modes computed by the DSC algorithm when the grid is 101^2) have less than 1 and 2% relative errors respectively. Such results are reliable for most practical purposes. It is also found that the DSC results of the first 70% modes are all subject to $<6\%$ relative errors, which might not be very reliable, but can be still useful for predicting the trend of high-frequency vibrations. Extensive convergence studies indicate that the DSC algorithm is insensitive to the changes in boundary conditions and internal support conditions, e.g., SCCS, CCCS and CCCC plates, which do not admit the Levy solution, exhibit the same convergence pattern as that of three solvable plates. Therefore, the DSC solutions are of benchmark quality for these unsolvable two-span plates and are recommended for checking potential numerical methods for the analysis of high-frequency vibrations.

ACKNOWLEDGMENT

This work was supported by the National University of Singapore and by the University of Western Sydney.

REFERENCES

1. R. S. LANGLEY and N. S. BARDELL 1998 *The Aeronautical Journal* **102**, 287–297. A review of current analysis capabilities applicable to the high frequency vibration prediction of aerospace structures.
2. D. C. ZHU 1985 In *Proceedings of the International Conference on Computational Mechanics*, May 1985, Tokyo. Development of hierarchal finite element methods at BIAA.

3. N. S. BARDELL 1991 *Journal of Sound and Vibration* **151**, 263–289. Free vibration analysis of a flat plate using the hierarchical finite element method.
4. O. BESLIN and J. NICOLAS 1997 *Journal of Sound and Vibration* **202**, 633–655. A hierarchical functions set for predicting very high order plate bending modes with any boundary conditions.
5. Y. XIANG, K. M. LIEW and S. KITIPORNCHAI 1996 *Acta Mechanica* **117**, 115–128. Exact buckling solutions for composite laminates: proper free edge conditions under in-plane loadings.
6. K. M. LIEW, C. M. WANG, Y. XIANG and S. KITIPORNCHAI 1998 *Vibration of Mindlin Plates, Programming the p-Version Ritz Method*. Amsterdam: Elsevier.
7. T. M. WANG and T. A. KINSMAN 1971 *Journal of Sound and Vibration* **14**, 215–227. Vibration of frame structures according to the Timoshenko theory.
8. J. R. BANERJEE and F. W. WILLIAMS 1994 *Computers and Structures* **50**, 161–166. An exact dynamic stiffness matrix for coupled extensional–torsional vibrations of structural members.
9. S. S. MESTER and H. BENAROYA 1995 *Shock and Vibration* **2**, 69–95. Periodic and near-periodic structures.
10. D. J. MEAD 1996 *Journal of Sound and Vibration* **190**, 495–524. Wave propagation in continuous periodic structures: research contributions from Southampton.
11. R. H. LYON 1975 *Statistical Energy Analysis of Dynamical Systems: Theory and Applications*. Cambridge, MA: MIT Press.
12. A. J. KEANE and W. G. PRICE 1987 *Journal of Sound and Vibration* **117**, 363–386. Statistical energy analysis strongly coupled systems.
13. R. S. LANGLEY and F. M. KHUMBAH 1995 *36th Structures, Structural Dynamics, and Material Conference*, New York: AIAA. Prediction of high frequency vibration levels in built-up structures by using wave intensity analysis.
14. G. W. WEI 1999 *Journal of Chemical Physics* **110**, 8930–8942. Discrete singular convolution for the solution of the Fokker–Planck equations.
15. G. W. WEI 2000 *Journal of Physics A: Mathematics and General* **33**, 4935–4953. A unified approach for the solution of the Fokker–Planck equations.
16. G. W. WEI 2000 *Journal of Physics A: Mathematics and General* **33**, 8577–8596. Wavelet generated by using discrete singular convolution kernels.
17. L. SCHWARTZ 1951 *Théore des Distributions*. Paris: Hermann.
18. G. W. WEI 2000 *Journal of Physics B* **33**, 343–352. Solving quantum eigenvalue problems by discrete singular convolution.
19. G. W. WEI 2001 *Computer Methods in Applied Mechanics and Engineering* **190**, 2017–2030. A new algorithm for solving some mechanical problems.
20. G. W. WEI 2001 *Physical Review Letters* **86**, 3542–3545. Synchronization of single-side averaged coupling and its application to shock capturing.
21. S. GUAN, C.-H. LAI and G. W. WEI 2001 *Physica D* **151**, 83–98. Bessel–Fourier analysis of patterns in a circular domain.
22. G. W. WEI 2000 *Physica D* **137**, 247–259. Discrete singular convolution method for the sine-Gordon equation.
23. M. J. ABLOWITZ, B. M. HERBST and C. SCHOBER 1996 *Journal of Computational Physics* **126**, 299–314. On numerical solution of the sine-Gordon equation.
24. G. W. WEI 1999 In *Computational Mechanics for the Next Millennium* (C. M. Wang, K. H. Lee and K. K. Ang, editors), 1049–1054. Amsterdam: Elsevier. A unified method for computational mechanics.
25. G. W. WEI 2001 *Journal of Sound and Vibration* **244**, 535–553. Vibration analysis by discrete singular convolution.
26. G. W. WEI 2001 *Engineering Structures* **23**, 1045–1053. Discrete singular convolution for beam analysis.
27. G. W. WEI, Y. B. ZHAO and Y. XIANG 2001 *International Journal of Mechanical Sciences* **43**, 1731–1746. The determination of the natural frequencies of rectangular plates with mixed boundary conditions by discrete singular convolution.
28. Y. B. ZHAO, G. W. WEI and Y. XIANG 2001 *International Journal of Solids and Structures* **39**, 1361–1383. Plate vibration under irregular internal supports.
29. Y. B. ZHAO, G. W. WEI and Y. XIANG 2002 *International Journal of Solids and Structures* **39**, 65–88. Discrete singular convolution for the prediction of high frequency vibration of plates.
30. S. TIMOSHENKO, D. YOUNG and W. WEAVER 1974 *Vibration Problems in Engineering* New York: John Wiley & Sons.
31. S. P. TIMOSHENKO and S. WOINOWSKY-KRIEGER 1970 *Theory of Plates and Shells* Singapore: McGraw-Hill.

32. R. D. MINDLIN 1951 *Transactions of the American Society of Mechanical Engineers Journal of Applied Mechanics* **18**, 31–38. Influence of rotatory inertia and shear on flexural motions of isotropic, elastic plates.
33. J. N. REDDY 1984 *Transactions of the American Society of Mechanical Engineers Journal of Applied Mechanics* **51**, 745–752. A simple higher-order theory for laminated composite plates.
34. I. DAUBECHIES 1992 *Ten Lectures on Wavelets*, *CBMS-NSF*, *Regional Conferences Series in Applications of Mathematics*, Vol. 61. Philadephia, PA: SIAM.
35. G. STRANG and T. NGUYEN 1996 *Wavelets and Filter Banks*. Wellesley, Massachusetts: Wellesley-Cambridge Press.
36. Y. XIANG, Y. B. ZHAO and G. W. WEI *International Journal of Mechanical Sciences*, in press. Levy solutions for vibration of multi-span rectangular plates.